Universiteit Utrecht

Department of Physical Geography

Modelling the effect of reservoirs on the suspended sediment flux of the Mississippi River

Master Thesis

Vera Zaremba

Supervisors:
Dr. Rens van Beek
Prof. Dr. Hans Middelkoop

Final Version

Utrecht, May 2018

Abstract

Before human interference the Mississippi River system transported on average approximately 400 MT/yr of suspended sediment to the Gulf of Mexico. In the last decades this transport has declined to only 110 MT/yr. The primary cause for this decline is the construction and implementation of human modifications to the river system. These human modifications include: the removal of obstacles, channel straightening, dikes, revetments, levees, floodways, dams and reservoirs. The decline in suspended sediment transport has resulted in the degradation of wetlands and coastal zones, extensive land loss and increased flood risks in the delta, which will only become more severe in the future as a result of climate change, subsidence and sea-level rise. This research focuses on the construction of dams and reservoirs as this is the primary source of suspended sediment reduction.

In this thesis the effect of the construction of reservoirs on the suspended sediment transport is analyzed by developing a quantitative model of the suspended sediment flux using the hydrological model PCR-GLOBWB. PCR-GLOBWB incorporates the hydrologic system of the Mississippi River Basin (MRB) and the reservoirs, for this research the model was extended to include suspended sediment deposition, transportation and trapping. The model was run for two end-member scenarios that included the 'initial' conditions without any reservoirs and the present conditions with all reservoirs. The results of the scenario with reservoirs were compared to previous research to validate the performance of the model. Furthermore, the temporal and spatial variability between the model output with and without reservoirs were analyzed to identify the effect of reservoir construction on the suspended sediment flux. The model was also run for three specific scenarios that included the removal of selected reservoirs in the tributaries and the main channels. These scenarios included the removal of nine main stem Missouri reservoirs, 34 large reservoirs (with a surface area of more than 100 km^2) and nine main stem Ohio reservoirs. These scenarios were run to identify the effect of the removal of selected dams of the suspended sediment flux and provide possible management options.

The relative error between the literature and the model output was primarily caused by the assumption that the sediment production of an entire subcatchment was constant in space and time. Furthermore, the model did not make a distinction between different types of erosion and therefore neglects the effect of local differences and extreme conditions. The year-to-year variability and seasonal variability in suspended sediment transport declined significantly if the reservoirs were introduced due to the storage capacity of the reservoirs, which resulted in a more constant discharge by lowering the peak discharges and increasing the minimum discharges. The greatest decline in sediment transport could be seen along the main channel of the Missouri and Lower-Mississippi, while the decline in the tributaries was less apparent. The sediment production in the Great Plains is the main source of suspended sediment which is independent of reservoir construction, however less of the available sediment is routed downstream if the reservoirs were introduced. The removal of the nine main stem Missouri reservoirs generated the largest increase in suspended sediment transport in comparison to the scenario that includes all reservoirs.

Acknowledgements

The completion of this MSc Research would not have been possible without the help and support of many people, both inside and outside Utrecht University. First of all I would like to thank my supervisors, Rens van Beek and Hans Middelkoop, for all the help, advice and support. I would especially like to thank Rens for the help and development of PCR-GLOBWB and the support on Phyton and PCRaster. Secondly, I would like to thank Pascal and Christa for peer reviewing my thesis, the much needed lunch breaks, coffee and support. Finally I would like to thank Zev for the patience when I was stressed and the tea he made me every night that I was working on my Thesis.

Vera Zaremba

Utrecht,

May 2018.

Contents

List of Figures

List of Tables

Chapter 1

Introduction

The Mississippi River is one of the most regulated rivers in the world, which is mainly the result of the construction and implementation of human modifications in the last decades. The effect of human modifications on the suspended sediment transport in the Mississippi is described by many articles and studies (Blum and Roberts (2009); Kesel (2003); Keown, Dardeau and Causey (1986); Meade and Moody (2010); Mossa (1996)). These modifications include several types of river engineering structures that have resulted in major benefits for transportation and navigation, generation of hydropower, flood control and many other factors. The implemented river engineering structures and measures include removal of obstacles, channel straightening and cutoffs, revetments, dikes, levees and floodways and dams and reservoirs. This research focuses on the construction of dams and reservoirs as this is the primary source of the reduction in sediment flux (Keown et al. (1986); Kesel and Yodis (1992); Meade and Moody (2010); Horowitz (2010)).

For example, Meade and Moody (2010) state that the sediment flux of the Missouri-Mississippi River system has significantly declined over the past century, from 400 MT/y before 1900 to an average 110 MT/y in the period 1987 to 2006 measured at Tarbert Landing (Figure 1.1). The authors state that the principal cause for this decline in suspended sediment is the construction of dams and reservoirs. Sediment trapping reduces the storage capacity and life-time of reservoirs. As a result of the decline in suspended sediment transport, the Mississippi delta experiences increased land loss and an increase in flood risk due to the loss of barrier islands, marshes and swamps, which form natural barriers against storm surges (Blum and Roberts (2009); CPRA (2017)). This thesis focuses on the Mississippi River as the recent decline in sediment transport is substantial, well documented and the principal cause is reservoir construction. Furthermore, restoring the pre-reservoir sediment flux could be the solution to the increased land loss and flooding in the Mississippi delta. Although extensive research has been done on the decline in sediment transport in the Mississippi River and its effects on the delta, not yet any successful attempts have been made to develop a quantitative model of the suspended sediment flux in the Mississippi and its tributaries on a catchment scale.

The main objective of this research is to analyze the effect of the construction of reservoirs on the suspended sediment transport in the Mississippi River Basin (MRB) by developing a quantitative model of the suspended sediment flux using the PCR-GLOBWB model. PCR-GLOBWB is a grid-based model of global terrestrial hydrology and water resources coded in Phyton and PCRaster-routines developed at Utrecht University (Van Beek & Bierkens, 2009). PCR-GLOBWB already incorporates the hydrologic system of the MRB and the reservoirs, for this research PCR-GLOBWB was extended to include sediment deposition, transportation and trapping. As the hydrologic parameters of the MRB are already incorporated in PCR-GLOBWB a limited number of input data is needed for the model extension, which can be obtained from existing literature and datasets such as the Global Reservoir and Dam dataset (GRanD), which incorporates the

location and main specification of 6862 dams and reservoirs.

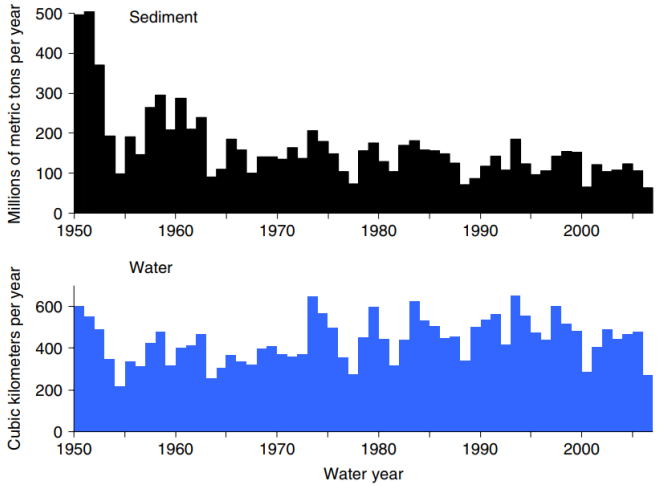

Figure 1.1: Annual sediment load and discharge in Mississippi measured at Tarbert Landing (Meade & Moody, 2010).

The following sub questions need to be addressed to achieve the main objective:

1. What is the most appropriate equation for the calculation of sediment trapping in the Mississippi reservoirs at this large scale based on literature studies and validation with case studies?
2. How do the results of the extended PCR-GLOBWB model compare in quantity and variability with previous research concerning suspended sediment transport in the Mississippi River Basin?
3. What is the effect of the construction of reservoirs on the temporal and spatial variability of the suspended sediment transport in the Mississippi River Basin?
4. Will the removal of selected dams and reservoirs result in an increase in sediment transport in the Mississippi? If so, which combination of reservoirs results in the highest increase in transport?

Firstly, a literature study on two separate subjects was conducted; the first chapter summarizes the existing literature on the sediment budget of the Mississippi River system (Chapter 1). The second chapter evaluates previous research concerning different methods to quantify sediment trapping in reservoirs (Chapter 2). Subsequently, the extension of PCR-GLOBWB to incorporate sediment transport and sediment trapping in reservoirs and the development of different scenarios will be explained (Methods). These scenarios include two end-members that incorporate the 'initial' conditions without any reservoirs and the present conditions with all reservoirs and three specific scenarios that include the removal of selected reservoirs in the tributaries or main river. The output of the model can be used to evaluate the basin wide effect of the introduction of reservoirs on sediment transport in the Mississippi River system. Furthermore, the output of the different scenarios can be used to identify the largest sediment sinks and provide solutions to the declining suspended sediment flux in the MRB. The model output will be analyzed on a basin wide and local scale and validated using results of previous research (Results). Subsequently, the results of the model runs will be discussed and possible recommendations for further research will be provided (Discussion). Finally, the conclusions that can be drawn based on this study will be summarized (Conclusion).

Chapter 2

Suspended sediment transport in the Mississippi River Basin

The first section of this chapter describes the general setting, characteristics, discharge distribution, suspended sediment sources and fluxes before human interference and reservoir characteristics. Subsequently, the decline in suspended sediment flux over time as a result of reservoir construction is described. The final section describes the effects of the declining suspended sediment load on the Mississippi River and Delta.

2.1 The Mississippi River Basin

2.1.1 Physical setting

The Mississippi drainage basin has a catchment area of approximately 3.2×10^6 km^2 and a total length of 3766 kilometers from its source at Lake Itasca (Minnesota) to the Gulf of Mexico (Figure 2.1). The watershed of the Mississippi extends from the Allegheny Mountains in the east to the Rocky Mountains in the west (Knox, 2007). The Mississippi can be divided in two sections: the Upper Mississippi, flowing from the source at Lake Itasca to the confluence with the Ohio River at Cairo and the Lower Mississippi, flowing from the confluence with the Ohio River to the Gulf of Mexico. Approximately 130 kilometers upstream of Baton Rouge, one fourth of the discharge of the Lower Mississippi is diverted through the Old River outflow channel into the Atchafalaya River, which is fed by the Red and White Rivers. The aim of the construction of the Control Structures was to control the diversion of the Mississippi water into the Atchafalaya River. Moody and Meade (2003) researched the effect of the Old River Control structures on the suspended sediment transport in the Mississippi and concluded their influence on the decline in sediment load at Tarbert Landing is negligible. The Lower Mississippi and Atchafalaya River discharge a combined average of 580 km^3/yr into the Gulf of Mexico (Meade, 1996). The Lower Mississippi has a length of approximately 1600 km and is one of the most intensely regulated rivers of the world. The MRB can be divided in 6 sub-catchments: the Missouri, Upper-Mississippi, Ohio, Arkansas, Red and Lower-Mississippi (Knox, 2007). The relative distribution of the drainage basin into the sub-catchments is presented in Figure 2.2. In this research the Red and Arkansas catchments are merged into one large catchment that incorporates the influence of the Red, White and Arkansas River.

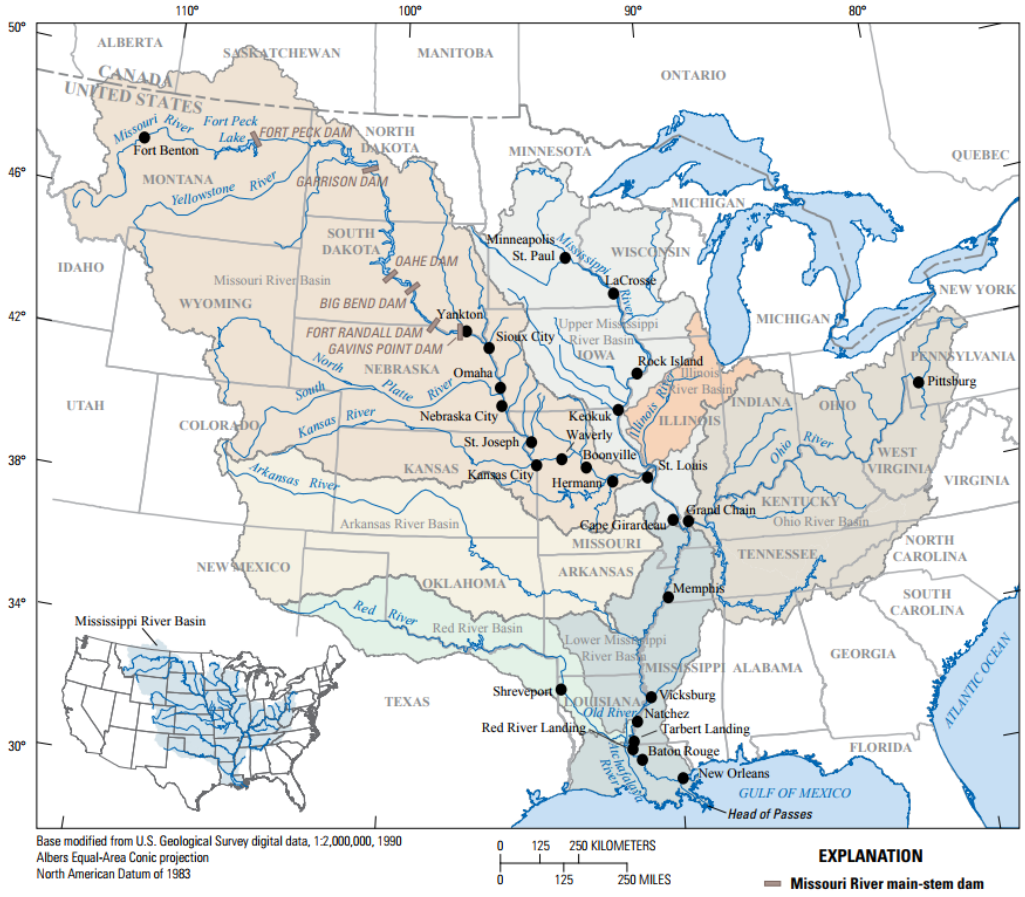

Figure 2.1: The Mississippi River Basin (Alexander et al., 2012).

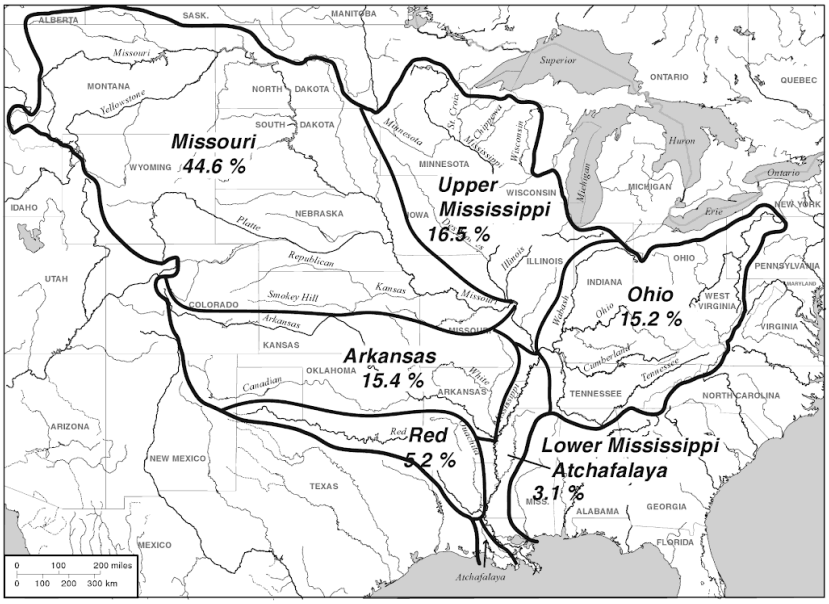

Figure 2.2: The subdivision of the MRB in 6 sub-catchments (Knox, 2007).

2.1.2 Climate and Discharge

The climate in the eastern half of the Mississippi drainage basin (Upper Mississippi, Ohio and main valley of the lower Mississippi basins) is relatively humid, while the climate in the western half (Missouri, Arkansas and Red River sub drainage basins) is semiarid. The annual precipitation depth is presented in Figure 2.3, the precipitation depth decreases in northern direction and from East to West. Most of the Missouri and Arkansas River catchments have a relatively low annual precipitation depth (<600 mm) in comparison to the Ohio River catchment, which has an average annual precipitation depth of more than 1000 mm (Court, 1974).

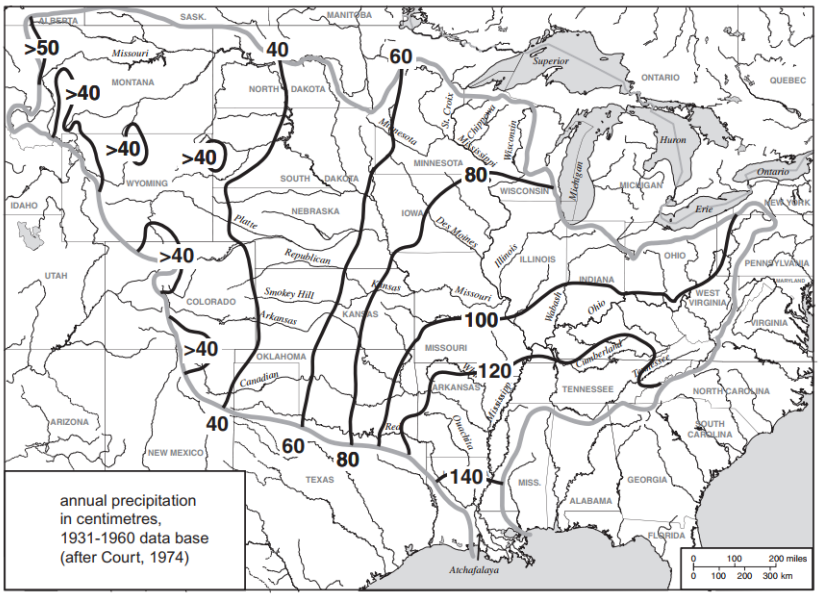

Figure 2.3: Annual precipitation depth in centimeters of the Mississippi drainage basin 1931-1960 (Court, 1974).

The low precipitation depth and the semiarid climate in the western half of the Mississippi drainage basin results in a low average annual runoff. The average annual runoff pattern is similar to the annual precipitation pattern. The runoff depth declines from East to West and in the northern direction from an average annual runoff depth ranging from 10 to 300 mm in the upper Mississippi River basin to a range of 300 to 600 mm in the Ohio River basin. The western border of the Mississippi drainage basin (located at the Rocky mountain front) shows a deviation in the annual runoff pattern, generating exceptionally high runoff depths ranging from 100 to 300 mm (Knox, 2007). The large differences in precipitation and runoff depths result in an asymmetrical and incongruent spatial discharge pattern. The Ohio River accounts for only 15.2 % of the total drainage area, but delivers nearly half of the total discharge at the mouth of the Mississippi, while the Missouri drains 44.6 % of the total drainage area, but contributes only 12 % of the total discharge at the mouth (Meade & Moody, 2010). This asymmetrical spatial discharge pattern can also be observed from Figure 2.4, which shows the average annual flood peak for the Ohio, Missouri and Lower-Mississippi River. Although the drainage area of the Missouri is approximately 1,36 million km^2 the largest flood magnitude since the year 1900 was approximately 22,000 m^3/s, while the largest flood magnitude of the Ohio River with a catchment of only 0,24 million km^2 was approximately 30,000 m^3/s.

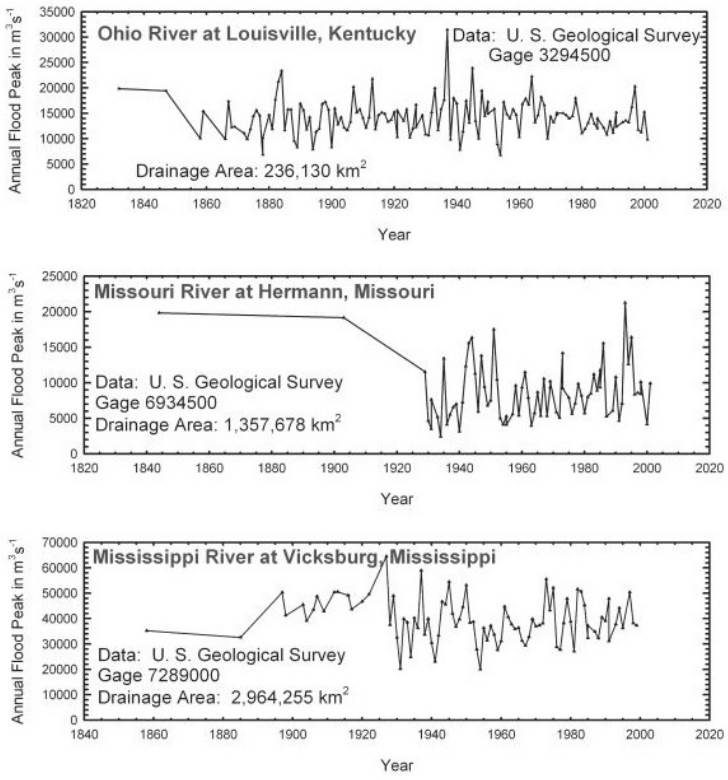

Figure 2.4: Annual average flood peak in m^3/s of the Ohio, Missouri and Lower-Mississippi River (Knox, 2007).

The construction of dams and reservoirs has resulted in a reduction in the occurrence of flood peaks and flow variability in the downstream river discharge. In general the discharge regulation is smaller in regions with abundant runoff and modest water use requirements (such as the Tennessee and Ohio River). A more severe reduction in flow variability can be observed in the Missouri River (Figure 2.5), which drains a drier catchment with low average annual runoff (Knox, 2007). Furthermore Figure 2.5 shows a slight increase in low stage flows to assist navigation and transportation.

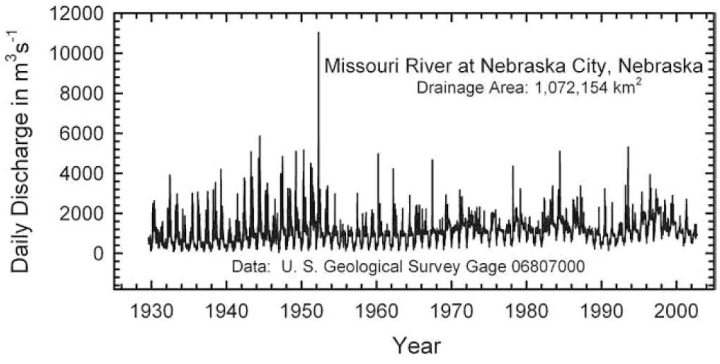

Figure 2.5: Average daily discharge in m^3/s for the period 1930-2006 of the Missouri River at Nebraska City (Knox, 2007).

2.1.3 Suspended sediment sources and loads before human interference

The primary sediment source of the Mississippi River are the northern Great Plains, rather than the less readily erodible Rocky Mountains and Appalachians. The Great Plains are underlain with a bedrock material that is composed of shales and siltstones that can easily be eroded by small to moderate amounts of rainfall. As a result of the large sediment yield generated by the Great Plains, the Missouri River is the primary sediment source of the Mississippi. Prior to the construction of human modifications and cultural development in the Mississippi River Basin, the suspended-sediment load that entered the Gulf of Mexico from the Mississippi and Atchafalaya River was approximately 394 MT/yr (Keown et al., 1986). This high suspended sediment yield was the result of the high rates of channel migration, erosion and bank calving (Kesel, 2003).

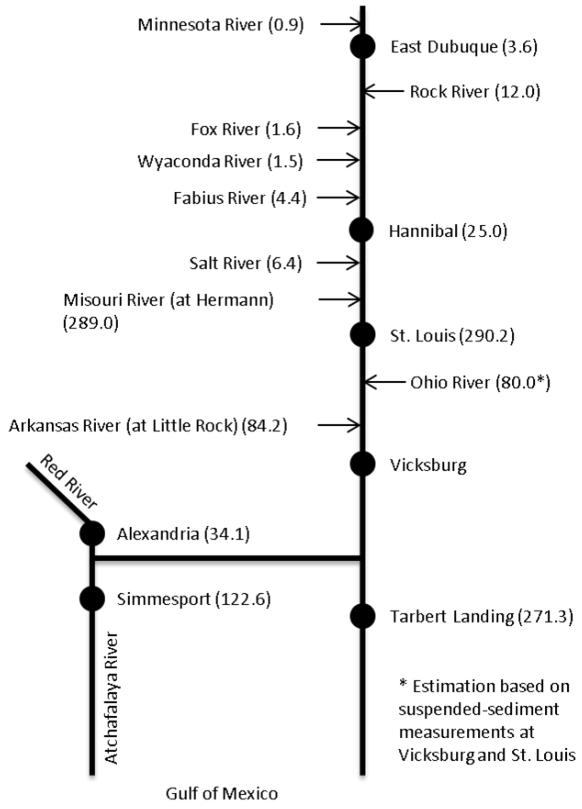

Figure 2.6: Suspended sediment load of the Mississippi prior to dam and reservoir construction around the year 1950 in MT/y derived from Keown et al. (1986).

Keown et al. (1986) described the suspended sediment regime before the construction of dams and reservoirs around the year 1950. There should however be noted that the suspended sediment load of the Mississippi was already declining before this year as a result of soil conservation practices, land use changes and dredging, the effect of these practices was however minor in comparison to the construction of dams and reservoirs. Keown et al. (1986) derived suspended sediment data from the database of the U.S. Army Engineer Waterways Experiment Station (USAEWES), which has collected, summarized and published sediment records since 1930 (USAEWES (1930) ; USDA (1954)). An overview of their results and measurements is presented in Figure 2.6. The suspended sediment load of the Mississippi was relatively low between Lake Itasca and the confluence with the Minnesota River. The Minnesota River discharged an average annual suspended sediment load of 0.9 MT/yr into the Upper Mississippi. Downstream from the confluence with the Minnesota River, the Mississippi received suspended sediment from many smaller tributaries, such as the

Rock, Fox, Wyaconda, Fabius, Salt and Illinois Rivers. However, these tributaries were of minor importance compared to the contribution of many streams in the western Mississippi River Basin. The sediment load of the Upper Mississippi was dominated by its confluence with the Missouri River at St. Louis, which provided an average sediment load of approximately 289 MT/y (at Hermann) before the construction of dams and reservoirs. The measurements of the suspended sediment load at Hermann (Missouri), St Louis (at confluence) and Hannibal (Upper-Mississippi) reflect the influence of the Missouri on the Upper-Mississippi sediment flux.

The lower Mississippi origins at Cairo were the Ohio River discharges into the Upper-Mississippi. The Ohio River contributed approximately 60 % of the total water discharge at the mouth of the Mississippi before human interference, but did not deliver a significant amount of sediment. The annual average suspended sediment yield of the Ohio River was approximately 80 MT/yr, which is not very significant in comparison to the 290 MT/yr delivered by the Upper Mississippi. The biggest sediment contributor in the Lower Mississippi is the Arkansas River, which provided approximately 84.2 MT/yr before human interference. The sediment flux of the other tributaries between Cairo and the confluence of the Arkansas and Lower Mississippi are minor and mostly unknown.

2.1.4 Reservoirs

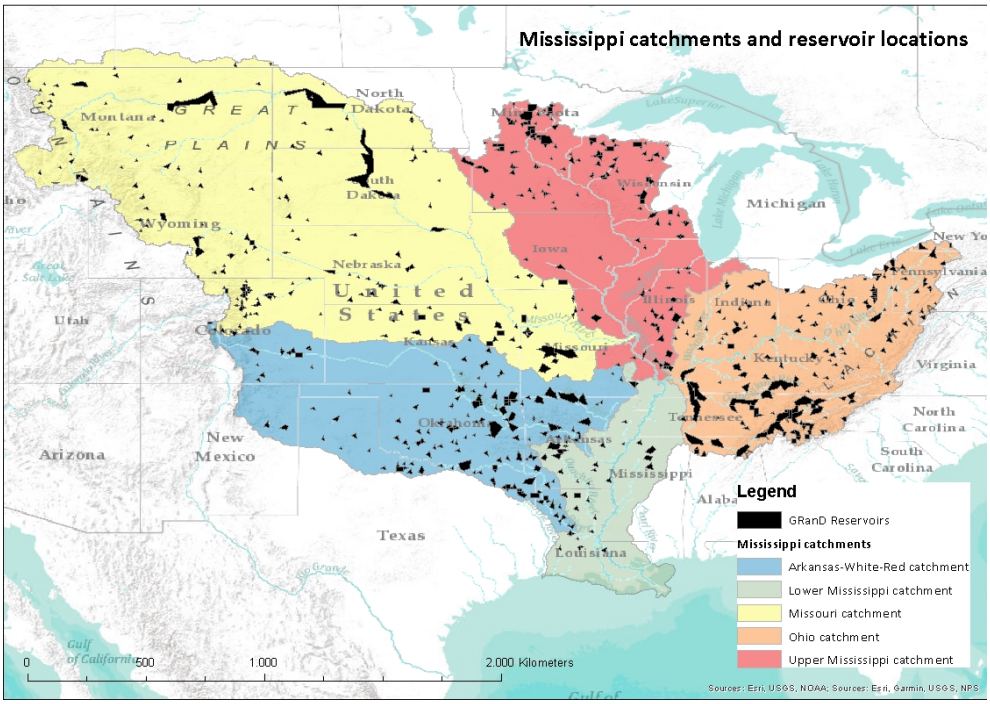

Figure 2.7: An overview of the sub-catchments (derived from the Watershed Boundary Dataset (WBD)) and reservoir locations in the MRB (derived from the GRanD database (Lehner et al., 2011)).

As stated in the introduction, dam and reservoirs construction resulted in a major decline in suspended sediment transport along the Mississippi and its tributaries. Dams and reservoirs were constructed with the aim to stabilize, harness and regulate the river flow and discharge, which is necessary for irrigation, agriculture, fresh water supply, transportation and navigation, fish and wild life habitat, flood control, water quality and recreation (Alexander et al., 2012). The Mississippi River system also incorporates many lock and dam structures, the primary purpose of

locks is to maintain sufficient water depth upstream of the lock for shipping. The construction of the lock and dam structures has increased transport via water from 30 million tons in 1940 to 400 million ton in 2011. At present, there are 21 lock and dam structures in the Ohio River, 18 in the Arkansas River and 5 in the Red River (Alexander et al., 2012). Figure 2.7 provides an overview of the different catchments in the MRB and the locations of the reservoir and dam structures. The reservoir data is derived from the Global Reservoir and Dam dataset (GRanD)(Lehner et al., 2011), which contains the location and main specifications of large global reservoirs with a storage capacity of more than 0.1 km^3 (a more detailed description of this dataset can be found in the method section). According to the GRanD database the Mississippi catchment incorporates 713 reservoir and dam structures with a total capacity of $330 * 10^9\ m^3$.

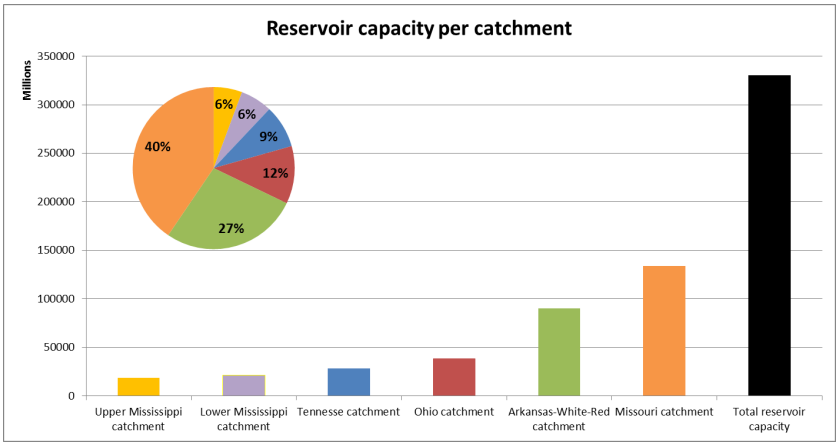

Figure 2.8: Overview of reservoir capacity per catchment in million cubic meter and percentages derived from the GRanD database (Lehner et al., 2011).

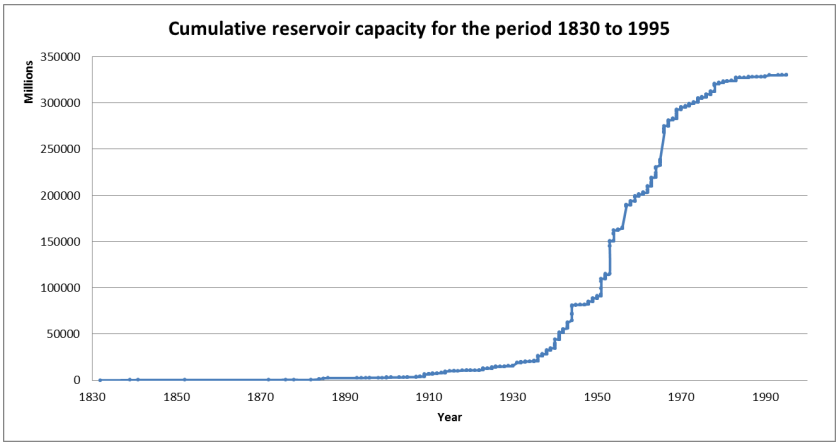

Figure 2.9: Cumulative reservoir capacity in million cubic meters over time derived from the GRanD database.

An overview of the reservoir capacity per catchment is presented in Figure 2.8 and the cumulative reservoir capacity over time is presented in Figure 2.9. Figure 2.8 shows that most of the reservoir capacity is located in the Missouri catchment, which contains 195 of the 713. The Upper-Mississippi catchment contains 149 of the reservoirs, but it contributes only 6% to the total reservoir capacity. From Figure 2.9 the conclusion can be drawn that most reservoirs became operational in the period between 1950 and 1970. The effect of the construction of these reservoirs in this period can clearly be observed in the Missouri River discharge (Figure 2.4 and 2.5).

2.2 The effect of dams and reservoirs on the suspended sediment flux

Meade (1996) states that the construction of dams and reservoirs in the Missouri and Arkansas River combined resulted in a 50 % decrease in the annual suspended sediment load of the Mississippi since the arrival of the first European settlers. The decline in suspended sediment transport is mainly the result of sediment trapping in the reservoir and behind the dams (Alexander et al., 2012). Large river systems such as the Mississippi are extremely complex in space and time. Over time the river system responds to changes in natural stressors, primarily climate, that result in changes in channel morphology depending on geomorphological and geological settings. The construction of dams and reservoirs and other engineering practices is superimposed on this natural complexity, although the effect of recent engineering projects can already be seen, it may take decades to see their entire coarse (Alexander et al., 2012).

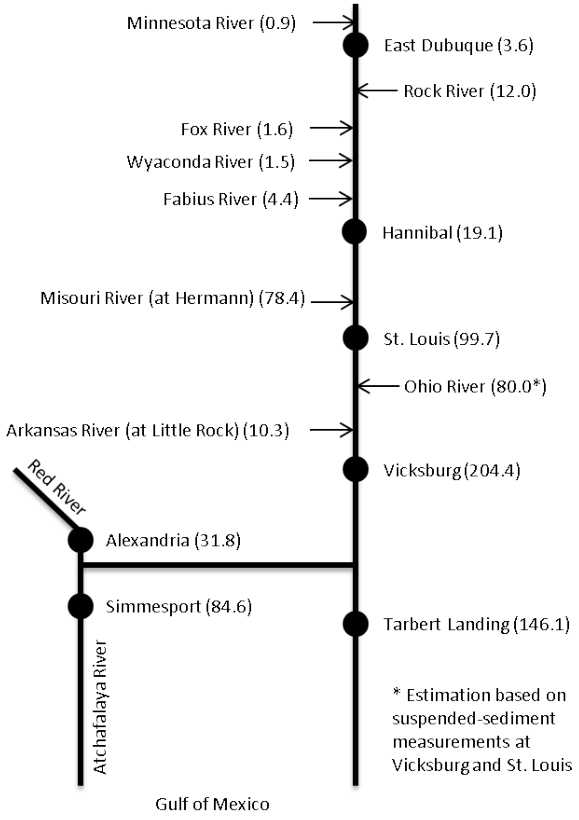

Figure 2.10: The suspended-sediment regime for the period 1970-1978 after human interference in MT/yr derived from Keown et al. (1986).

Keown et al. (1986) described the suspended-sediment flow regime of the Mississippi after the construction of most reservoirs and dams (Figure 2.9) for the period 1970-1978 (Figure 2.10), which can be compared to the situation prior to construction in Figure 2.6. This comparison demonstrates that the Missouri delivered 289 MT/yr prior to human modifications and only 78.4 MT/yr in the period 1970-1978 and the Arkansas River delivered 84.2 MT/yr prior to human modifications and only 10.3 MT/yr in the period 1970-1978.

2.2.1 The Missouri River dams

Many scientific articles (Keown et al. (1986); Kesel and Yodis (1992); Meade and Moody (2010); Horowitz (2010)) state that the construction and closure of the Missouri dams is the primary source of the reduced annual suspended sediment transport in the Mississippi River. Meade and Moody (2010), described the effect of the construction of the dams and reservoirs in the Missouri River on the Mississippi River system by comparing the decline in suspended sediment transport at several measurement stations in the Missouri with the decline measured at Tarbert Landing (Figure 2.11). The closure of the Fort Randall dam in 1953 resulted in a major decline in the suspended sediment load at Yankton (South Dakota), from 160 MT/yr per year in 1952 to approximately 50 MT/yr in 1953. The construction of the Gavins Point Dam in 1955 just upstream from Yankton, resulted in a decline in sediment load to an annual average of 10 MT/yr. The construction of the Fort Randall and Gavins Point Dam thus resulted in a total decline of suspended sediment load of approximately 150 MT/yr. The annual suspended sediment transport at Hermann (last measurement location before the confluence of the Missouri and Mississippi) is significantly higher than the sediment load at Yankton and Omaha, this is the result of the sediment input of several tributaries. However, the influence of these tributaries has diminished in recent years due to the introduction of soil-conservation practices (Parker, 1988).

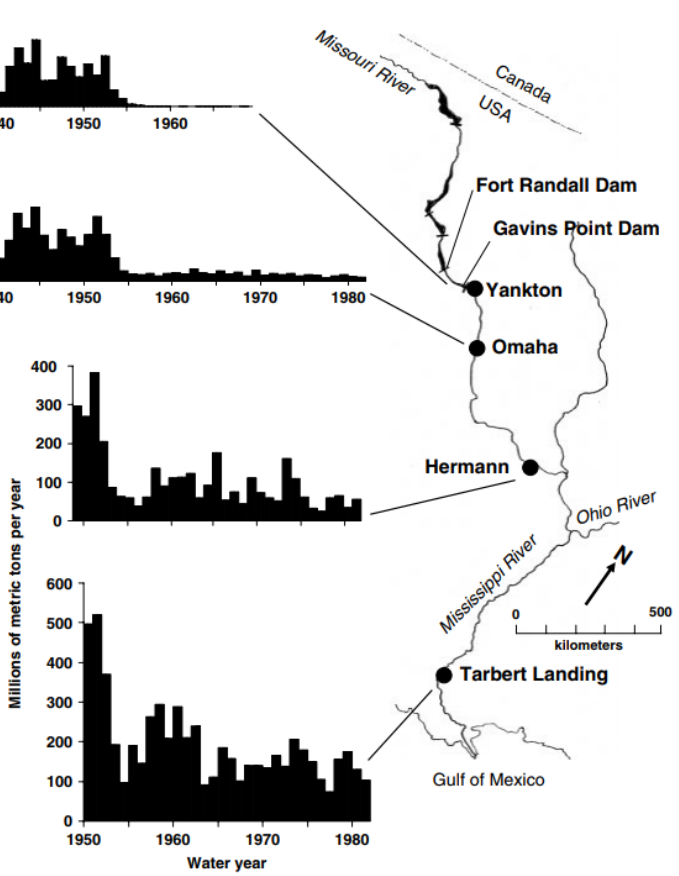

Figure 2.11: Suspended-sediment load in million metric tons per year measured at Yankton, Omaha and Hermann in the Missouri River and Tarbert Landing in the Mississippi River (Meade & Moody, 2010).

The decline in suspended sediment load measured at Tarbert Landing is approximately 200-300 MT/yr, which is significantly larger than the decline measured at Yankton. A steep decline in

annual average sediment transport can be seen at Tarbert Landing in the period between 1951 and 1954. This steep decline is the result of the decrease in annual discharge in this period, as the year 1951 was a year of record flooding while the year 1954 was extremely dry. Therefore, the annual average sediment transport would have shown a more gradual decline in this period if there had been a more constant discharge. The large difference in annual sediment load between Hermann and Tarbert landing (100-200 MT/yr) in the period 1950-1981 is the result of remobilization of older fluvial sediments that were stored in the long-term storage sites (along the meandering channel and in the meandering belt) along the Mississippi between St Louis and Tarbert Landing. Another reason for the large difference is the contribution of the Upper-Mississippi and the Ohio River to the suspended sediment transport at Tarbert Landing. The difference between Hermann and Tarbert Landing became smaller in the late 1960s and 1970s, which indicates the long-term storage sites were depleted (Meade & Moody, 2010).

2.3 Other sources of sediment decline

2.3.1 Land use changes

Since the beginning of the 1930s the U.S. Government has initiated soil conservation programs to counteract the rapidly increasing soil loss rates. The soil conservation practices included contour plowing, construction of small sediment-retention dams on higher order streams, replanting vegetation and stabilization of stream banks (Keown et al., 1986). According to Meade and Moody (2010) a part of the long-term slow decline in suspended discharge is due to the reduction of soil erosion in the uplands of the source regions. However, because the imprints of the soil conservation practices occur gradually their effects are obscured by the construction of reservoirs in the 1950s and early 1960s.

2.3.2 Revetment construction

As described in the previous section, most sediment in the Lower-Mississippi was generated by the high rate of bank calving. The construction of revetments has resulted in a reduction of over 90% in the bank calving rate. The cumulative kilometers of revetment construction and the related decrease in bank calving rate are presented in Figure 2.12, the figure shows that the rate of bank calving significantly declined between the period 1877-1892 and 1965-1972.

2.3.3 Sediment trapping in dike constructions

Another source of suspended sediment flux reduction is the accretion of sediment in dike constructions, on the Lower-Missouri this accounts for approximately 14% of the total decline in mean annual suspended sediment transport in the period 1910-1981 (Jacobson, Blevins & Bitner, 2009). Kesel (2003) reported that a similar rate of land accretion around dikes can be found in the Lower-Mississippi, indicating that in the period of dike construction land accretion may have accounted for a substantial part of the basin wide decline in suspended sediment load. However, at present the trapping efficiency of the dike constructions is negligible, as they have already accreted a substantial volume of sediment ((Alexander et al., 2012).

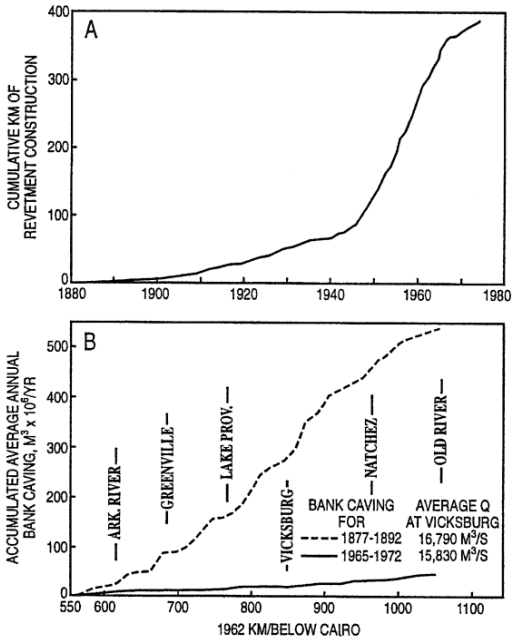

Figure 2.12: (A) History of revetment construction in the Vicksburg district, (B) Average annual accumulated bank calving rate before and after revetment construction (Kesel, 2003).

2.4 Effect of declining sediment flux on Mississippi River and Delta

2.4.1 Disconnection river channel-floodplain

The construction of dams and reservoirs has resulted in a substantial reduction of the peak flow magnitude, which can be observed throughout the entire Mississippi (Galat & Lipkin, 2000). Furthermore, the reduction in suspended sediment transport, redirection of flow towards the channel by dike construction and dredging has caused a lowering in channel bed elevation due to scouring (Jacobson et al., 2009). The construction of levees, lowering of the river bed elevation and the reduced peak flow magnitude caused a disconnection between the river channel and the floodplain, except during extreme flood events. Prior to human modifications the floodplains and wetlands were flooded semiannually, providing the ecosystem with sediment and nutrients. As a result of the loss in sediment and nutrient supply, the wetlands and coastal zones can no longer counteract the forces of subsidence, sea-level rise and storm surges, resulting in land loss (Paola et al., 2011).

2.4.2 Drowning of the Mississippi Delta

The decline in suspended sediment flux of the Mississippi River has had major consequences for the Mississippi delta, which is confronted with an increasing rate of land loss. Sediment storage in the alluvial-deltaic plain is primarily dependent on the suspended sediment flux and the accommodation space. The accommodation space is created by sea-level rise and subsidence. Blum and Roberts (2009) predicted two future trends in land loss rate based on a relative sea-level rise of 1 mm/yr and based on an accelerated sea-level rise from 3 mm/yr in 2000 to 4 mm/yr in 2100. The upper and lower limits of the land loss trends are defined by different subsidence scenarios, in which the lower limit presents higher subsidence rates than the higher limit.

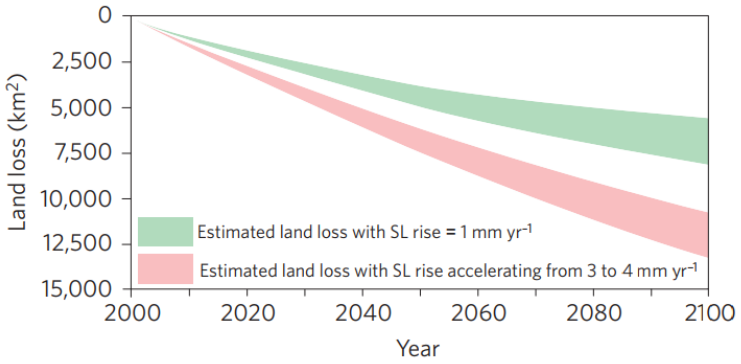

Figure 2.13: Estimated land loss for the Mississippi delta region up to the year 2100 (Blum & Roberts, 2009).

Furthermore, Blum and Roberts (2009) predicted the sediment mass balance up to the year 2100 based on four different scenarios of relative sea-level rise and suspended sediment supply. The first scenario assumed the modern suspended sediment flux of the Mississippi, a trapping efficiency of 40% and a sea-level rise of 1 mm/yr. In this scenario the creation of accommodation space is greater than the sediment supply resulting in a mass deficit of approximately 1 to 5 billion tons by the year 2100. If the sea-level rise accelerated from 3 mm/yr in 2000 to 4 mm/yr in 2100 the sediment mass balance deficit will be as much as 11-17 billion tons in 2100. The authors also constructed a scenario in which they assumed an increase in suspended sediment transport to pre-dam conditions (400-500 MT/y). With a sea-level rise of 1 mm/yr the sediment supply to the delta would be sufficient to sustain the submergence of the deltaic plain, if the sea-level is accelerated this would however still result in a mass deficit of 3-9 billion tons by the year 2100.

2.4.3 Increasing Flood risks

The loss of barrier islands, marshes and wetlands has resulted in an increase in flood risk, as these ecosystems would normally reduce incoming storm surges. This enlargement in flood risks increases the vulnerability of communities and important navigation routes. Morton (2008) investigated the land loss on six different barrier islands in the Gulf of Mexico. Morton states that the principal causes for the loss in barrier islands are relative sea-level rise, the decline in suspended sediment supply and the increased frequency of intense storms. Furthermore, the author concludes that the reduction in sediment supply by the Mississippi is most likely the primary reason for the accelerated rates of land loss, as this is the only primary cause with a historical trend that temporally matches the trend of barrier island land loss.

2.4.4 A Future Without Action

The Coastal Protection and Restoration Authority of Louisiana (CPRA) developed a master plan for a sustainable coast ((CPRA, 2012) ; (CPRA, 2017)) with the aim to build a coastal protection and restoration strategy for the next 50 years. The master plan describes a scenario for a future without action, as the implementation of many projects will not happen in the coming years. The 'Future Without Action' scenario describes the conditions that would occur throughout coastal Louisiana if no further action is taken to sustain and protect the coast and without a change in the suspended sediment flux. The CPRA developed a low, medium and high scenario based on the changes in environmental drivers (Appendix 1), in which the precipitation, evapotranspiration, sea-level rise, subsidence rate, storm frequency and average storm intensity are included (more

information about the climate scenarios can be acquired from Appendix C of the Coastal Master Plan of 2017). Figure 2.14 shows the potential land loss over the next 50 years with the current suspended sediment flux and different environmental scenarios.

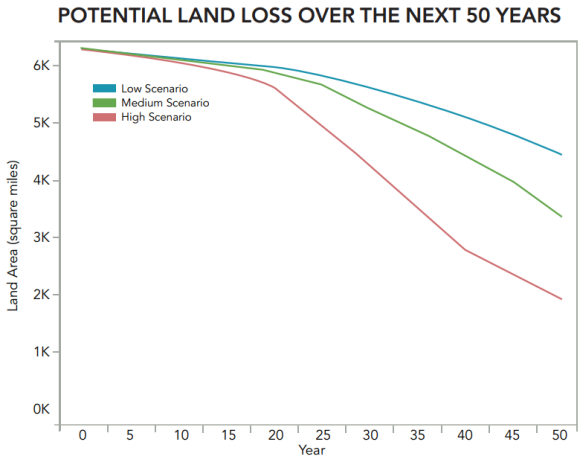

Figure 2.14: Range of potential land loss for all scenarios that Louisiana would experience without action over the next 50 years (CPRA, 2017).

The Coastal Master Plan introduces the construction of sediment diversions as a primary solution to counteract the increasing land loss rate. Sediment diversions are structures or new channels that transport water, sediment and nutrients to the wetlands counteracting submergence and land loss. Research of Kim et al. (2009) modelled the expected land creation initiated by the construction of two sediment diversions at Mid-Breton and Barataria, which are currently in the designing phase. From the modeling study could be concluded that 700 to 900 km^2 of land could be created by the year 2110 if the diversion sites have a trapping efficiency of 40%, experience an average sea-level rise and have a 45% access to the Mississippi sediment load.

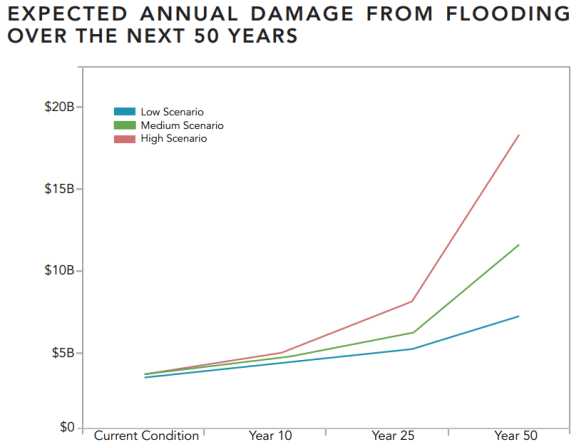

Figure 2.15: Expected annual damage from flooding for the different climate scenarios (CPRA, 2017).

The Future Without Action scenario also takes into account the increase in flood risk, flood depth and predicted future inundation from a 100-year flood event. The increase in flood risk is mainly the result of the loss in natural defenses, such as barrier islands. Figure 2.15 presents the expected

annual damage from flooding events and the flood depths over the next 50 years. Figure 2.15 starts at the expected annual damage under initial conditions, which is approximately $2,7 million dollars per year, in 50 years these annual costs could increase to $6,7 million for the low scenario and to as much as $12 million for the high scenario.

Chapter 3

Studying sediment trapping in reservoirs

This chapter focuses on describing the mechanisms behind sediment trapping in reservoirs and the different methods by which this can be quantified.

3.1 Sediment trapping

In the last century, mankind has constructed more than 45,000 dams (higher than 15m) on Earth, with the primary aim to control temporal variations in water supply and demand. Although the primary aim of these reservoirs is to regulate and capture streamflow, they all, no matter their size, shape or function, result in sediment deposition. Sediment trapping reduces the storage capacity and life time of reservoirs and is a major carbon sink (Verstraeten & Poesen, 2000). In most cases, the sedimentation in reservoirs occurs at a faster rate than the loss of integrity of the dam structure. The life time of the reservoir is therefore usually controlled by the rate of sedimentation (Wisser et al., 2013). Hargrove et al. (2010) concluded that sedimentation in many US reservoirs has reduced their life time 50 to 100 years. The rate of sedimentation in reservoirs is site specific and controlled by several factors, resulting in large global differences and uncertainties. Many articles state that the most effective way to characterize sediment trapping in a reservoir is the trapping efficiency (TE) (Brown (1944); Brune (1953); Heinemann (1981)), which is defined as the relative fraction of the incoming sediment that is deposited or trapped in the reservoir. This relative fraction (or TE) can be calculated by dividing the sediment mass that is deposited in the reservoirs ($S_{deposited}$) by the sediment mass that entered the reservoir (S_{in}). The deposited sediment mass can also be quantified by subtracting the outflowing sediment mass (S_{out}) from the inflowing sediment mass (Verstraeten & Poesen, 2000) (Equation 3.1).

$$TE = \frac{S_{deposited}}{S_{in}} = \frac{(S_{in} - S_{out})}{S_{in}} \tag{3.1}$$

Figure 3.1 presents an overview of the parameters that influence the trapping efficiency of a reservoir. Of primary importance are the settling velocity and retention time that control the sedimentation process. The settling velocity is mainly dependent on the particle size, which influences the settling velocity, and water chemistry, which influences the particle size distribution by flocculation. The retention time of a reservoirs is dependent on the characteristics of the inflow hydrograph and the geometric characteristics of the reservoir. Due to the many different factors that influence the TE of a reservoir it is hard to establish an empirical relation. Theoretically, all

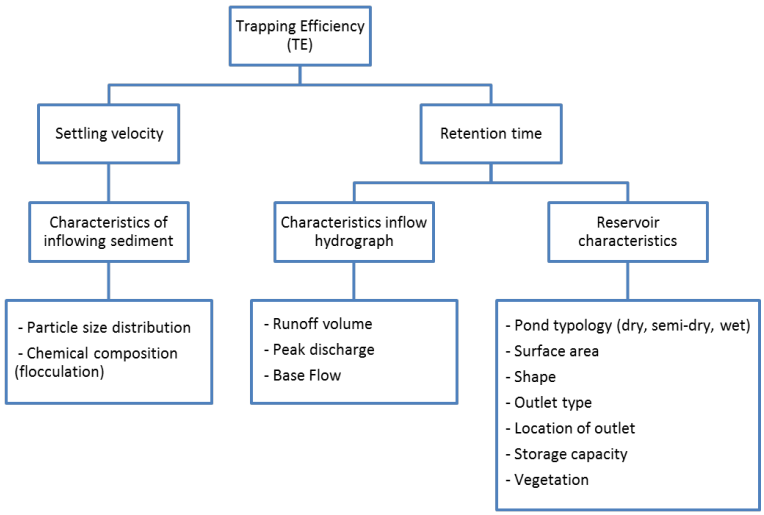

Figure 3.1: Different factors that influence the trapping efficiency of a reservoir (derived from (Verstraeten & Poesen, 2000)).

factors should be included in the calculation of the TE, this would however require very complex data and an extensive availability of input parameters. In this research a simplified method will be used to determine TE based on the available reservoir data. The next sections describe various empirical and theoretical methods that were used in previous research to quantify TE.

3.2 Empirical models predicting trapping efficiency

The described empirical methods quantify TE based on an independent parameter (capacity/inflow (C/I) ratio and sedimentation index (S.I.)), which is a dynamic variable. Therefore, there should be noted that the independent parameter declines over time as a result of sedimentation in the reservoirs and the related decline in storage capacity. Furthermore, the presented TE curves may not represent the actual long-term annual average as they are based on empirical data that can deviate with the frequent occurrence or lack of extreme events during the period of data collection.

3.2.1 Determining TE using the capacity-annual inflow ratio

Brune (1953) developed a curve that relates the trapping efficiency to the capacity-annual inflow ratio based on the data of 40 normally ponded US reservoirs (i.e. reservoirs that have an outlet at the top of the embankment and are completely filled)(Figure 3.2). This method takes into account both the relative capacity of the reservoir (C) and the annual inflow generated by runoff from the watershed (I). Furthermore, the C/I ratio provides information on the type of reservoir, if the C/I ratio is greater than 1 the reservoir can be classified as a hold-over storage reservoir, whereas the ratio is 1 or less the reservoir can be classified as a seasonal storage reservoir (i.e. reservoir capacity is replaced annually). The C/I ratio therefore also represents the average residence time of the water in the reservoir, a higher C/I ratio represents a longer residence time and hence a higher fraction of sediment deposition.

The curve derived by Brune (Figure 3.2) shows the sediment trapping efficiency in percent against the C/I ratio. The figure shows an envelope around the mean curve, where the upper bound corresponds to highly flocculated and coarse sediments, while the lower bound corresponds to

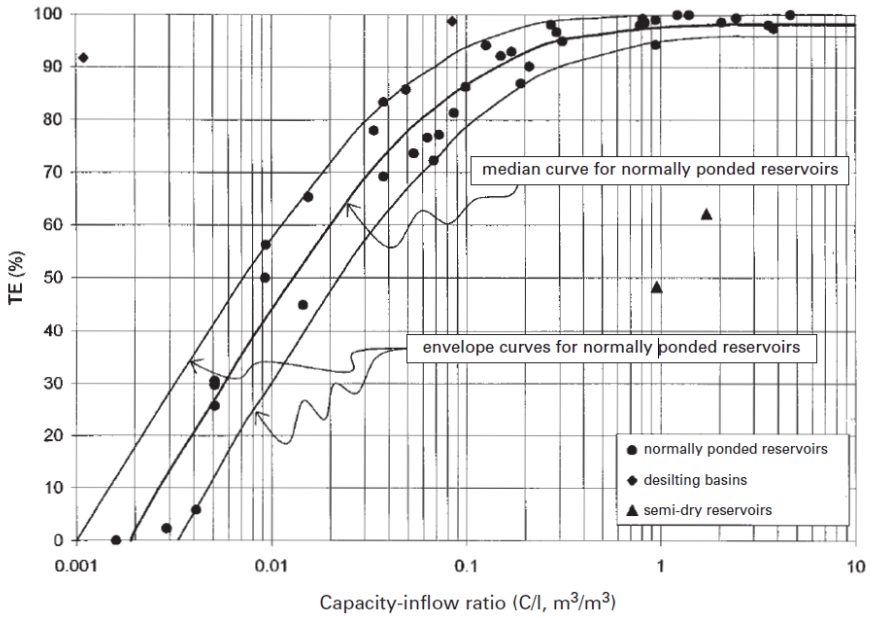

Figure 3.2: Trapping efficiency as related to the capacity/inflow ratio (Brune, 1953).

colloidal, fine-grained sediments. In theory the trapping efficiency of a reservoir could never be equal to zero or 100 %, as this would mean that the storage capacity or runoff would reduce to zero or become infinitely large. However, the trapping efficiency of a reservoir could be very close to 100 % if there are no water losses over spillways or through outlets. Furthermore, Brune concluded that a negative trapping efficiency could occur for reservoirs with a very low C/I value, as these reservoirs may alternatively fill and scour depending on stream flow conditions. The following conclusions were drawn on the assumption that the reservoir is a normally ponded reservoir, which is a reservoir that is completely filled by water and has an outlet at the top of the embankment. Desilting basins (i.e a structure placed directly downstream of a diversion structure designed to trap sediment) probably have much higher trapping efficiencies as a result of their shape, while reservoirs located in semi-dry or dry environments probably have a much lower trapping efficiency.

Brune (1953) did not provide an algebraic equations to calculate TE based on the developed curves. Gill (1979) provided three equations (for coarse, medium and fine sediment) that closely fit the three curves proposed by Brune. For medium grained sediments Gill (1979) proposed the following equation:

$$TE = \frac{\frac{C}{I}}{0.012 + 1.02 \times \frac{C}{I}} \tag{3.2}$$

In which C represents the reservoirs capacity in m^3 and I represents the mean annual inflow in m^3/yr. Heinemann (1981) modified Brunes curve to quantify TE for smaller reservoirs and ponds using data from 20 normally ponded reservoirs located in the Tennessee Valley (USA) with a surface area that did not exceed 40 km^2. Heinemann concluded that his curve predicted smaller TE values for certain reservoirs than the TE curves derived by Brune (1953)(Figure 3.3). Heinemann (1981) provided the following equation relating the TE to the C/I ratio for small reservoirs and ponds (surface area $< 40 \quad km^2$):

$$TE = -22 + \frac{119.6 \times \frac{C}{I}}{0.012 + 1.02 \times \frac{C}{I}} \tag{3.3}$$

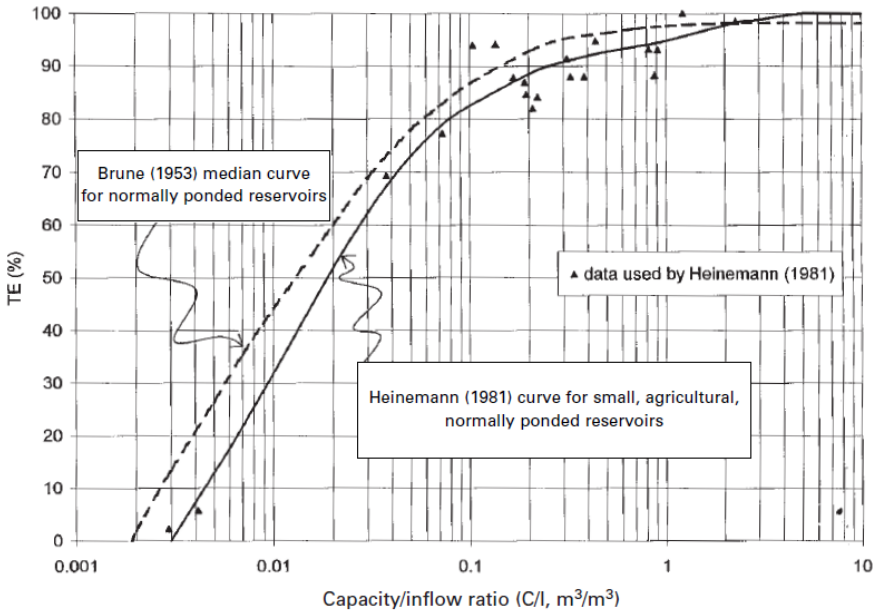

Figure 3.3: The curves derived by Brune (1953) and Heinemann (1981) relating TE to the C/I ratio (derived from Verstraeten and Poesen (2000).

Many articles (e.g. Vörösmarty et al. (2003); Kummu et al. (2010); Wisser et al. (2013)) quantify TE using the equation derived by Ward (1980) (Equation 3.4) to predict Brunes curve, as it provides reasonable estimates of long-term average trapping efficiency. Ward (1980) states that this simplified relation, based on the residence time (τ) of a reservoir, fits the US reservoir data of Brune reasonably well (down to C/I = 0.005).

$$TE = 1 - \frac{0.05}{\sqrt{\tau}} \rightarrow \tau = \frac{C}{I} \quad ratio \tag{3.4}$$

3.2.2 Determining TE using a sedimentation index

Churchill (1948) derived a relationship between the sediment passing through a certain reservoir (i.e. 100 – TE (%)) and a sedimentation index ($S.I.$)(Figure 3.4), which can be calculated by dividing the residence time (or C/I ratio) by the mean flow velocity through the reservoir (V).

$$S.I. = \frac{\tau}{V} = \frac{C/I}{V} \tag{3.5}$$

The mean flow velocity can be measured or estimated by diving the average inflow (I) by the cross-sectional area of the reservoir (A), which can also be derived by dividing the capacity (C) by the length of the reservoir (L).

$$V = \frac{I}{A} = \frac{I}{C/L} \tag{3.6}$$

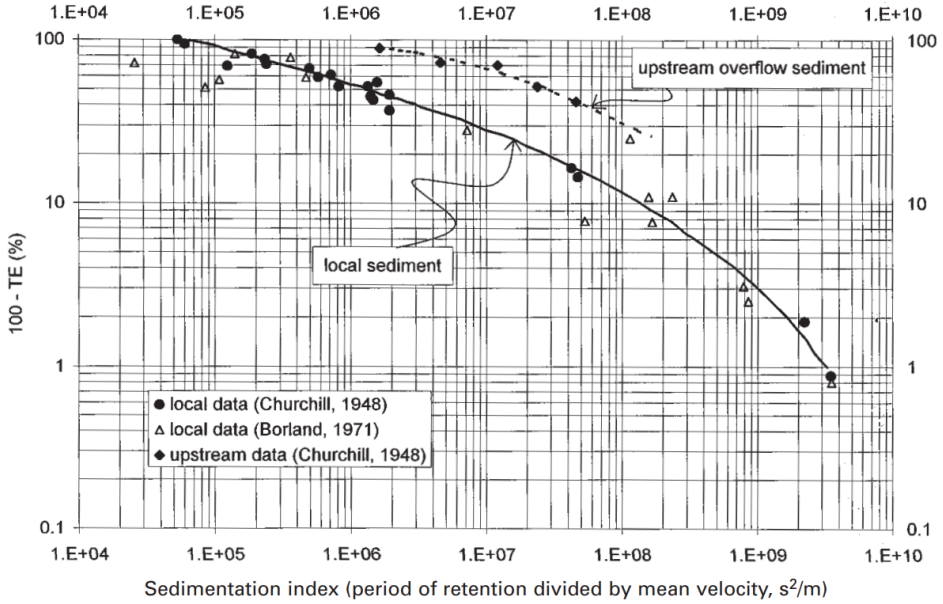

Figure 3.4: The curve derived by Churchill (1948) relating the sediment passing through the reservoir (100-TE(%)) to a sedimentation index (derived from Borland (1971)).

The equation for the sedimentation index can than be rewritten as:

$$S.I. = \frac{CA}{I^2} = \frac{C}{I^2} \times \frac{C}{L} = \frac{C/I^2}{L} \tag{3.7}$$

Churchill (1948) distinguished two different curves to predict TE, one for finer grained sediment discharged from overflow of upstream reservoirs and one for the 'local' coarser grained sediment originating from erosion in the catchment. As finer grained sediment originating from upstream reservoirs is less likely to deposit in the next reservoir (high settling velocity) than coarser grained 'local' material. Therefore, TE values are lower for reservoirs that have a sediment supply that largely originates from upstream reservoirs than TE values for reservoirs that have a sediment supply that originates from a local source. Borland (1971) applied Churchill's curve for data of desilting and semi-dry reservoirs and concluded that Churchill's approach is valid for these types of reservoirs, while Brune's curve is not. Although the method of Churchill takes into account the mean flow velocity in the reservoir and gives better predictions of TE than the method of Brune, Brune's method is more widely used than Churchill's method. This is the result of the lacking availability of input data for Churchill's method, which requires the average flow velocity or length of the reservoir.

3.3 Theoretical models predicting trapping efficiency

Theoretical models attempt to quantify TE based on the principles of particle sedimentation in water assuming steady discharge and varying flow conditions (quiescent or turbulent). Many articles (e.g. Verstraeten and Poesen (2000); Haan, Barfield and Hayes (1994)) also describe a theoretical approach to quantify TE under variable discharge conditions. The models and methods for variable discharge conditions are however very complex and require extensive reservoir data, these methods are therefore beyond the scope of this research.

3.3.1 Steady discharge and quiescent flow

The first theoretical modelling study was done by Camp (1945), who researched sedimentation in an ideal rectangular flow basin or settling tank. Camps model assumed quiescent flow with steady discharge conditions, complete mixing and no resuspension. When the sediment enters the ideal reservoir, it will settle down with a settling velocity (V_s) which is directly related to the particle size. In an idealized situation, the critical settling velocity (V_c) could be determined as the settling velocity of particles which are 100% removed from the settling tank. If the settling velocity is less than the critical settling velocity the sediment is deposited in the reservoir with the rate V_s/V_c. The relation between the settling velocity and the critical settling velocity is presented in Figure 3.5.

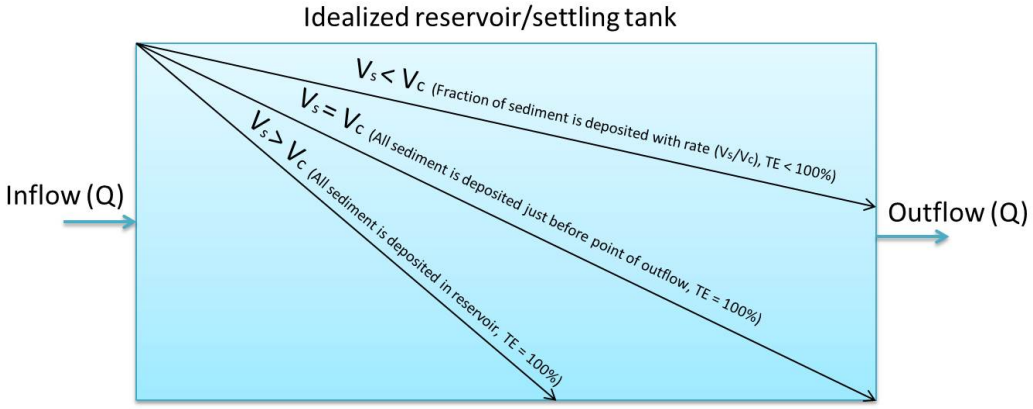

Figure 3.5: Sediment flow trajectories in an idealized reservoir with quiescent flow and steady discharge (derived from Haan et al. (1994)).

The critical settling velocity can be related to the overflow rate using the water depth (d), retention time (T), reservoir volume (v), surface area of the reservoir (A) and the in- or outflowing discharge (Q) (Haan et al., 1994) (Equation 3.8).

$$V_c = \frac{d}{T} = \frac{d}{(v/Q)} = \frac{d}{(d \times A)/Q} = \frac{dQ}{dA} = \frac{Q}{A} = overflow \quad rate \tag{3.8}$$

The settling velocity of the ideal flow basin can either be measured or estimated from existing literature. Subsequently, the TE can be calculated using the overflow rate:

$$TE = 100 \times \frac{V_s}{V_c} = 100 \times \frac{A}{Q} * V_s \tag{3.9}$$

3.3.2 Steady discharge and turbulent flow

Camp (1945) concluded that turbulence has a great effect on the sedimentation in a reservoir. Therefore Camp related the TE to a turbulence parameter. A more detailed description of this method can be found in Haan et al. (1994). Chen (1975) modified the TE equation of Camp to include the effects of turbulent flow, as ideal settling in reservoirs is not realistic. Chen proposed that sediment deposition under turbulent flow can be quantified based on the water velocity (V_w), critical velocity (V_c), settling velocity (V_s) and the sediment concentration (C) (Equation 3.10).

$$Deposition = \alpha \times V_s \times C \quad in \quad which \quad \alpha = \left(1 - \frac{V_w}{V_c}\right) \tag{3.10}$$

The concentration at time t can be calculated using the initial concentration ($C(0)$) channel depth (d):

$$C(t) = C(0) \times e^{-\left(\alpha \frac{V_s}{d}\right)t} \tag{3.11}$$

Subsequently, the TE can be quantified as:

$$TE = 100 \times \left[1 - e^{-\left(\alpha \frac{V_s}{d}\right)t}\right] = 100\left[1 - e^{-\left(\alpha V_s \frac{A}{Q}\right)t}\right] \tag{3.12}$$

Chen concluded that the greatest differences between quiescent and turbulent flow occur where the settling velocity is close to the critical settling velocity, because under quiescent flow the particles settle at these conditions while under turbulent flow these conditions will result in resuspension and outflow. Furthermore, Chen attempted to compare his results for the calculation of TE with the empirical results of Brune (1953) and Churchill (1948) (Figure 3.6). Chen concluded that the empirical curves underestimate TE for coarse sediments and overestimate TE for fine sediments.

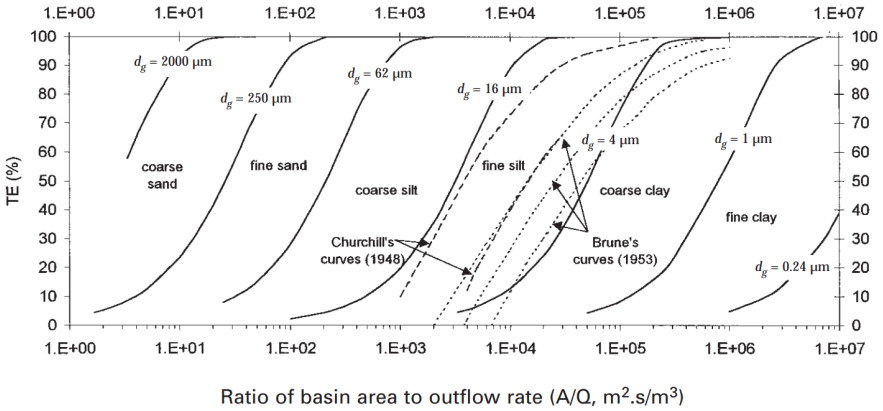

Figure 3.6: The TE curves of Chen (1975) for different grain sizes (d_g) compared to the empirical TE curves of Brune and Churchill (derived from Verstraeten and Poesen (2000))

Chapter 4

Research methods

4.1 PCRaster GLOBal Water Balance model (PCR-GLOBWB)

PCR-GLOBWB is a grid-based model of global terrestrial hydrology developed by the Department of Physical Geography of the University of Utrecht (Van Beek and Bierkens (2009)) . The concept model is presented in Figure 4.1. PCR-GLOBWB calculates the water storage and exchange in two soil layers (Store 1 and Store 2) and a groundwater layer (Store 3) for each grid cell on a daily basis. Furthermore, the model takes into account the water exchange fluxes between the layers and the atmosphere. The vertical fluxes between the stores include upward capillary rise fluxes ($Q_{2\rightarrow1}$ and $Q_{3\rightarrow2}$) and downward percolation fluxes ($Q_{1\rightarrow2}$ and $Q_{2\rightarrow3}$). The fluxes between the stores and the atmosphere are influenced by the presence of canopy and snow cover and include precipitation (PREC), evapotranspiration (E_{pot}) and snow accumulation and melt. The resulting local discharge along the channel ($Q_{channel}$) is depicted on the right side of Figure 4.1, including the effect of local gains and losses and lateral in- and outflow. $Q_{channel}$ is fed by the drainage components of the soil and groundwater layers, which consist of direct runoff (QDR), interflow (QSF) and base flow (QBF).

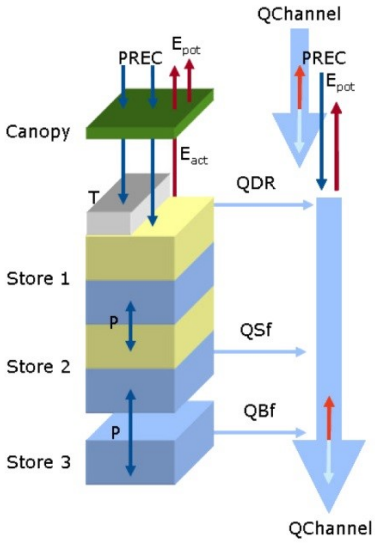

Figure 4.1: Model concept PCR-GLOBWB (Van Beek & Bierkens, 2009)

.

The surface water and surface water routing are included in the PCR-GLOBWB model as a separate land cover class, which subdivides the surface water into a network with river and lake stretches. The resulting river discharge and lake storage are mainly affected by precipitation, evaporation, water consumption and direct in and outputs to open water. The total runoff of the land surface is fed to the river network without delay before routing. PCR-GLOBWB uses a distributed flow routing model, which is based on partial differential equations that calculate the flow rate and water level as a function of space and time (Chow, Maidment & Mays, 1988). To this extent, discharge is calculated using the kinematic wave approximation of the Saint-Venant Equation, which assumes one-dimensional unsteady open channel flow (Van Beek & Bierkens, 2009). For the derivation of the Saint-Venant equation the following assumptions are made: flow is one-dimensional (1), the fluid is incompressible (2), the bottom slope of the channel is small (3), streamline curvature is small (4), hydrostatic pressure prevails and vertical accelerations can be neglected (5) and Manning's equation should be used to describe resistance effects (6).

The Saint-Venant equation consists of the continuity equation and the momentum equation:

$$\frac{\delta Q}{\delta x} + \frac{\delta A}{\delta t} = q \quad (continuity) \tag{4.1}$$

$$A = \alpha Q^{\beta} \quad (momentum) \tag{4.2}$$

In which Q is the discharge through the channel $[m/s]$, x is the length along the channel $[m]$, A is the channel cross-section $[m^2]$, t is the elapsed time [s], q is the inflow per length of channel $[m^2/s]$ and α and β represent empirical constants. The continuity and momentum equation can be combined into one governing equation:

$$\frac{\delta Q}{\delta x} + \alpha\beta Q^{(\beta-1)} * \frac{\delta Q}{\delta t} = q \tag{4.3}$$

The value of α and β can be obtained using Manning's equation (Chow et al., 1988):

$$Q = \frac{R^{\frac{2}{3}}\sqrt{S}}{n} A \tag{4.4}$$

Where S is the slope gradient $[m/m]$, n is the Manning's roughness coefficient $[-]$ and R is the hydraulic radius $[m]$, which can be calculated by dividing the surface area A $[m^2]$ by the wetted perimeter P $[m]$. In this research Manning's n was set at a value of 0.04 for the channels and at a value of 0.1 for the floodplains. The equation can be rewritten in terms of A with the substitution of R by A/P.

$$A = \left(\frac{nP^{\frac{2}{3}}}{\sqrt{S}}\right)^{\frac{3}{5}} * Q^{\frac{3}{5}} \tag{4.5}$$

From which can be deduces that:

$$\alpha = \left(\frac{nP^{\frac{2}{3}}}{\sqrt{S}}\right)^{\frac{3}{5}} \tag{4.6}$$

and

$$\beta = \frac{3}{5} \tag{4.7}$$

The wetted perimeter is dependent on the water level, as a lower water level results in a reduction in the value of P. Therefore, the calculated discharge of the previous time step is used to estimate a value for the wetted perimeter. PCR-GLOBWB uses an internal function of PCRaster which approximates a numerical solution of the Saint-Venant kinematic wave equation. The function takes into account the lateral inflow, the calculated value for α and β and the discharge of the previous time step to calculate the new discharge (Q_{t+1}) at every point along the channel. From the direct input to the freshwater surface and the total drainage from the land surface the lateral inflow to the channel can be calculated (Van Beek & Bierkens, 2009):

$$q = \frac{Q_{tot}}{\Delta L} = \frac{A_{cell}}{\Delta L}\left(\left[1 - Frac_{water}\right]\sum_{i}\left[Q_i + Frac_{water} * I_w\right]\right) \tag{4.8}$$

Where q represents the lateral inflow to the channel $[m^2/s]$, $Frac_{water}$ represents the fraction of open water surface within a cell, ΔL represents the length of the channel $[m]$, I_w represents the direct inputs to the freshwater surface $[m/d]$ and Q_i represents the interflow per m slope width $[m^2/s]$. The water level in the lakes and reservoirs was assumed to be static over time.

4.2 Adding the sediment component to PCR-GLOBWB

The PCR-GLOBWB model includes all the hydrologic components of the MRB. In this research the sediment production and transport along the Mississippi was added to PCR-GLOBWB to model the suspended sediment flux over time. The quantification of the trapping efficiency was added to the model to account for sediment deposition and transport in the reservoirs.

4.2.1 Sediment production

The sediment delivery and production of the tributaries to the Mississippi is variable per sub-catchment. Therefore, a constant sediment production rate was established for the different sub-catchments (Figure 2.2 or 2.7) using pre-reservoir suspended sediment loads. The pre-reservoir sediment loads were obtained from the research of Keown et al. (1986). The sediment production per sub-catchment was calculated by dividing the sediment load by the basin area of the sub-catchment (derived from the WBD). In this simulation, for each sub-catchment a steady sediment production and supply to the river was assumed to remove the uncertainties concerning the delivery ratio and local dynamics. The results per sub-catchment are presented in Table 4.1. The obtained production values were added to the Watershed Boundary dataset (WBD) map and converted to a raster dataset that could be used as input map for PCR-GLOBWB. The Tennessee and Ohio region were merged into one hydrologic unit with a uniform sediment production as the Tennessee River is the largest tributary of the Ohio River.

Table 4.1: Parameters required for deriving the sediment production per hydrologic unit.

Hydrologic Unit	Metric Tons	Basin Area (m^2)	Sediment Production ($kg/m^2/year$)
Missouri	$2.892*10^8$	$1.349*10^{12}$	0.214
Upper Mississippi	$3.289*10^7$	$4.920*10^{11}$	0.067
Ohio	$7.257*10^7$	$5.279*10^{11}$	0.137
Arkansas / Red / White	$1.217*10^8$	$6.422*10^{11}$	0.189
Lower Mississippi	$6.622*10^6$	$2.760*10^{11}$	0.024

4.2.2 Sediment transport

The transport capacity of the Mississippi and its tributaries is mainly dependent on the stream power and the particle density. The transport capacity $[kg/m^3]$ can be calculated using the equation developed by Govers (1990):

$$TC = \rho * c\Big[100(\omega - \omega_{cr})\Big]^d \tag{4.9}$$

Where ρ is the material density $[kg/m^3]$, ω is the unit stream power $[m/s]$, ω_{cr} is a critical threshold for the stream power and c and d are empirically derived coefficients. The derivation of c and d is the first step in the sediment modeling process. The value for c and d can be derived from the mean particle size D $[m]$ (Govers, 1990):

$$c = \left(\frac{D * 10^6 + 5}{0.32}\right)^{-0.6} \tag{4.10}$$

$$d = \sqrt[4]{\frac{D * 10^6 + 5}{300}} \tag{4.11}$$

Subsequently, the unit stream power (ω) can be calculated:

$$\omega = v * \sin\alpha \tag{4.12}$$

Where v is the flow velocity $[m/s]$ and α is the slope angle. The critical unit stream power indicates the limit below which no further sediment transport can occur. In this research, a default value of 0.004 m/s (as derived by Govers (1990)) was used. Woolhiser, Smith and Goodrich (1990) established that when the unit stream power is 0.004 m/s, Govers equation is no longer valid for small flow velocities. Therefore, they assumed a threshold unit stream power of 0.007 m/s below which a transitional relationship can be applied from $\omega = 0$ to $\omega = 0.007$ to calculate the actual transport capacity:

$$TC = \left(3 - \frac{2\omega}{0.007}\right) * \left(\frac{\omega}{0.007}^2\right) * TC_{\omega=0.007} \quad \text{if} \quad \omega \leq 0.007 \tag{4.13}$$

The transport capacity denotes the sediment load in kilograms per cubic meter, the total sediment load in the river is therefore also dependent on the discharge. The transport capacity is thus linked to the routing process described in the previous section. The sediment uptake and deposition are dependent on the sediment concentration and the transport capacity. The sediment concentration is based on the sediment load and the water storage (volume) and can be calculated via:

$$C_{sed} = \frac{S_{load}}{V} \tag{4.14}$$

in which C_{sed} is the sediment concentration $[kg/m^3]$, S_{load} is the sediment load $[kg]$ and V is the water volume of the cell $[m3]$. In principle, sediment uptake occurs if the sediment concentration is lower than the transport capacity and sediment deposition occurs if the sediment concentration is higher than the transport capacity. The rate of sediment uptake is different in the channels than in the reservoirs and lakes (water bodies), for this research, the sediment uptake in water bodies is assumed to be zero. The sediment uptake $[kg/s]$ in the channels is dependent on the sediment

uptake factor, which is assumed to be 1 [−] (S_{UF}), the discharge (Q) and the difference between TC and C_{sed}:

$$If \quad TC - C_{sed} > 0 \quad S_{uptake} = S_{UF} * (TC - C_{sed}) * Q \tag{4.15}$$

$$If \quad TC - C_{sed} < 0 \quad S_{uptake} = 0 \tag{4.16}$$

Sediment deposition in the channels is dependent on the difference between TC and C_{sed}, settling velocity (V_s) (Equation 4.21), channel width ($W_{channel}$) and the channel length ($L_{channel}$):

$$If \quad TC - C_{sed} > 0 \quad S_{deposition} = 0 \tag{4.17}$$

$$If \quad TC - C_{sed} < 0 \quad S_{deposition} = \Big(TC - C_{sed}\Big) * V_s * W_{channel} * L_{channel} \tag{4.18}$$

The channel width and channel length can be derived from the hydrologic parameters in PCR-GLOBWB (Leopold & Maddock, 1953). The channel width was derived directly from the attributes, while the channel length was derived from the square root of the surface area. The calculation of the settling velocity and the trapping efficiency is described in the next section. The sediment deposition in the water bodies is dependent on the trapping efficiency and the incoming sediment load:

$$S_{deposition}\big(\text{in waterbodies}\big) = -TE * S_{load} \tag{4.19}$$

The total sediment load is calculated for each cell and every time step, the equation is the same for channels and water bodies:

$$S_{tot} = \Big(S_{load} + S_{uptake} + S_{deposition}\Big) * \Delta T \tag{4.20}$$

For this research, all sediment load located in the water bodies was set to the outflow point, the remaining cells within the water body were set to zero. An overview of the used input parameters are presented in Table 4.2.

Table 4.2: Overview of used input parameters for PCR-GLOBWb model.

Parameter	Symbol	Unit	Value
Manning's roughness coefficient (channels)	n	−	0.04
Manning's roughness coefficient (floodplains)	n	−	0.1
Material density	ρ	kg/m^3	1000
Critical unit stream power	ω_{cr}	m/s	0.004
Threshold unit stream power	ω	m/s	0.007
Mean particle size	D	m	$5 * 10^{-6}$
Sediment uptake factor	S_{UF}	−	1

4.2.3 Calculating trapping efficiencies

Several reservoirs with a known trapping efficiency derived from previous research were used to established which of the methods described in Chapter 3 could best be used to quantify sediment trapping at a large scale. The equation developed by Camp (1945) provided the best results in comparison with other literature, and was therefore used as governing equation to quantify trapping efficiency in this research.

The equation derived by Camp is described in Section 3.3.1 and assumes sedimentation in an ideal rectangular continuous flow basin or settling tank and a steady discharge, quiescent flow, complete mixing and no occurrence of resuspension (Equation 3.9). This method is based on the difference between the settling velocity (V_s) and the critical settling velocity (V_c). The settling velocity used in this research was obtained from the research of Thonon et al. (2005) and calculated from the median grain size D [m]:

$$V_s(\text{settling velocity}) = aD^b = 710 * D^{1.57} \tag{4.21}$$

In this research, the constants a and b were given a value of 710 and 1.57 respectively and the median grain size was assumed $5 * 10^{-6}$ m (derived from the research of Thonon et al. (2005)). The settling velocity (V_s) was therefore assumed at $3.38 * 10^{-6}$ m/s. The critical settling velocity (V_c) is calculate from the reservoir surface area (A) derived from the GRanD database and the discharge (Q) derived from the PCR-GLOBWB model.

$$V_c(\text{critical settling velocity}) = \frac{Q}{A} \quad \text{(Equation 3.8)} \tag{4.22}$$

4.3 Overview of used databases

4.3.1 The Global Reservoir and Dam dataset (GRanD)

The GRanD database contains the location and main specifications of 6862 dams and reservoirs that have a storage capacity of more than 0.1 km^3 (Lehner et al., 2011). The GRanD dataset attributes contain the dam and reservoir names, name of the impounded river, spatial coordinates, year of construction, surface area, storage capacity, dam height, main purpose and elevation. Furthermore, the dataset provides an estimate of the long-term average discharge at all reservoir locations. The average discharge is obtained from linking the GRanD to the HydroSHEDS model, which is a near-global high resolution digital river network (Lehner, Verdin & Jarvis, 2008). For this research, the dams and reservoirs located in the MRB were extracted from the GRanD database using the clip geoprocessing tool in ArcMap. The clip function filters the dams and reservoirs located in the Mississippi catchment using a mask of the catchment. All overlapping values are selected and merged into a new layer.

4.3.2 USGS Sediment Data Portal

The USGS Sediment Data Portal was designed to help users identify, access and interpret suspended sediment and related data of the US. The Sediment Data Portal can be accessed via `https://cida.usgs.gov/sediment/`. The portal provides the opportunity to select measurement sites and download the site specific daily and discrete data on suspended sediment concentration, stream flow and site characteristics. This data portal was used to obtain suspended sediment concentrations (mg/L) at several locations directly upstream of reservoirs and downstream of dam constructions to verify and validate the outcome of the trapping efficiency calculations.

4.3.3 The Watershed Boundary Dataset (WBD)

The WBD defines the areal extent of surface water drainage to a point, accounting for all land and surface areas. The dataset can be downloaded via https://datagateway.nrcs.usda.gov and added as layer file to ArcGIS. The WBD was developed with the intent to define hydrologic units (or watersheds) to establish a base-line drainage boundary framework, accounting for all land and surface areas (Berelson, Caffrey & Hamerlinck, 2004). The boundaries of the hydrologic units are solely defined on science-based hydrologic principles, not accounting for administrative boundaries. For this research, the hydrologic units located in the MRB were extracted from the WBD using the clip geoprocessing tool in ArcMap. The clip function filters the hydrologic units located in the MRB using a mask of the catchment. All overlapping polygons are selected and merged into a new layer.

4.4 Developing scenarios

Several scenarios were developed to quantify the effect of the removal of selected dams and reservoirs on the suspended sediment flux. In the first scenario all reservoirs were removed, which represents the pre-human situation before construction. The opposite (second) scenario includes all the reservoirs, representing the present situation. These first two scenarios were developed to validate the model output with other research and establish a baseline to analyze the other scenarios. Many articles (e.g. Meade and Moody (2010); Horowitz (2010)) state that the construction of the Missouri River dams has resulted in the greatest decline in sediment transport and that removal of these dams could possibly solve the sediment shortages in the delta. Therefore, the scenario that removed the dams on the main stem of the Missouri was developed. The scenario that included the removal of the main stem Ohio dams was developed to evaluate if this would yield the same results as the scenario that removed the Missouri main stem dams. The scenario removing all large reservoirs with a surface area larger than 100 km^2 was chosen to evaluate if the decline in suspended sediment transport is primarily caused by sediment storage in large reservoirs. The removed reservoirs were identified using the GRanD database in ArcGIS. An overview of the developed scenarios is presented in Table 4.3 and Figures 4.2 and 4.3. In Appendix 2, an overview can be found of all the removed reservoirs per scenario based on the GRanD ID and dam/reservoir name. Table 4.4 presents the removed reservoirs capacity per scenario and the relative percentage in comparison to the total reservoir capacity in the MRB.

Table 4.3: Overview of scenario names, number of removed reservoirs and short description of excluded attributes.

Scenario	Number removed	Scenario name	Excluded attributes
1	713	No Reservoirs	No reservoirs are included
2	0	All Reservoirs	All reservoirs are included
3	9	Main Missouri Reservoirs removed	All main reservoirs in the Missouri River were removed
4	34	Large Reservoirs removed	All reservoirs with a surface area larger than 100 km^2 were removed
5	9	Main Ohio Reservoirs removed	All main reservoirs in the Ohio River were removed

Table 4.4: Overview of removed reservoirs capacity and the relative percentage in comparison to the total reservoirs capacity.

Scenario	Reservoir capacity removed $[km^3]$	Percentage removed
No Reservoirs	330.3	−100%
All Reservoirs	0	0%
Main Missouri Reservoirs removed	86.5	−26.2%
Large Reservoirs removed	187.5	−56.8%
Main Ohio Reservoirs removed	15.3	−4.6%

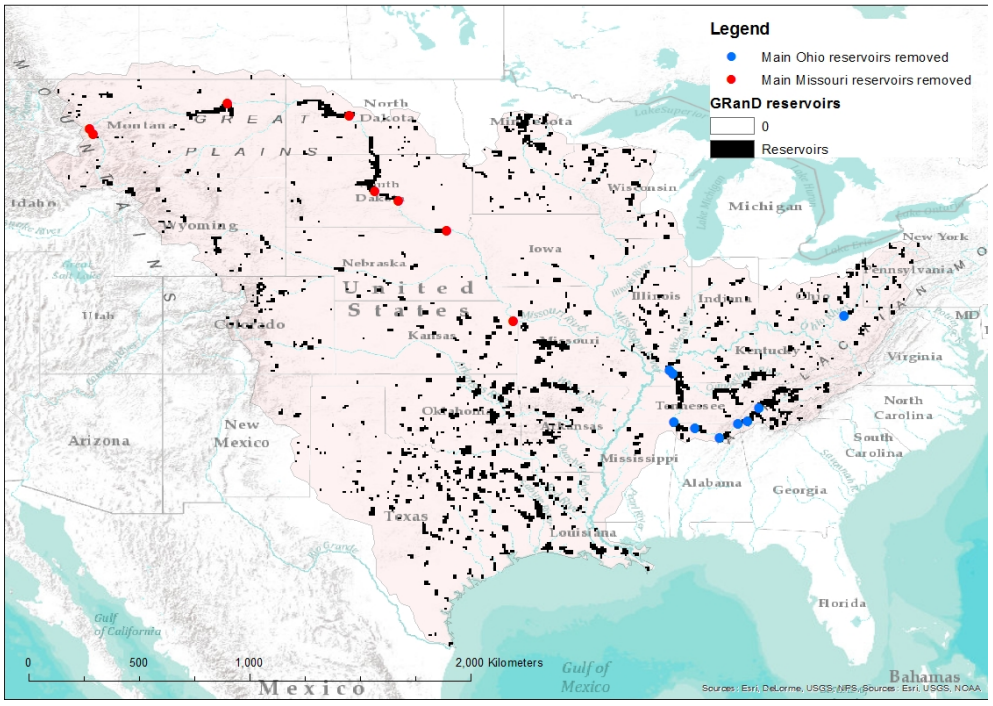

Figure 4.2: Overview map representing the scenario in which the main stem Missouri and Ohio reservoirs are removed.

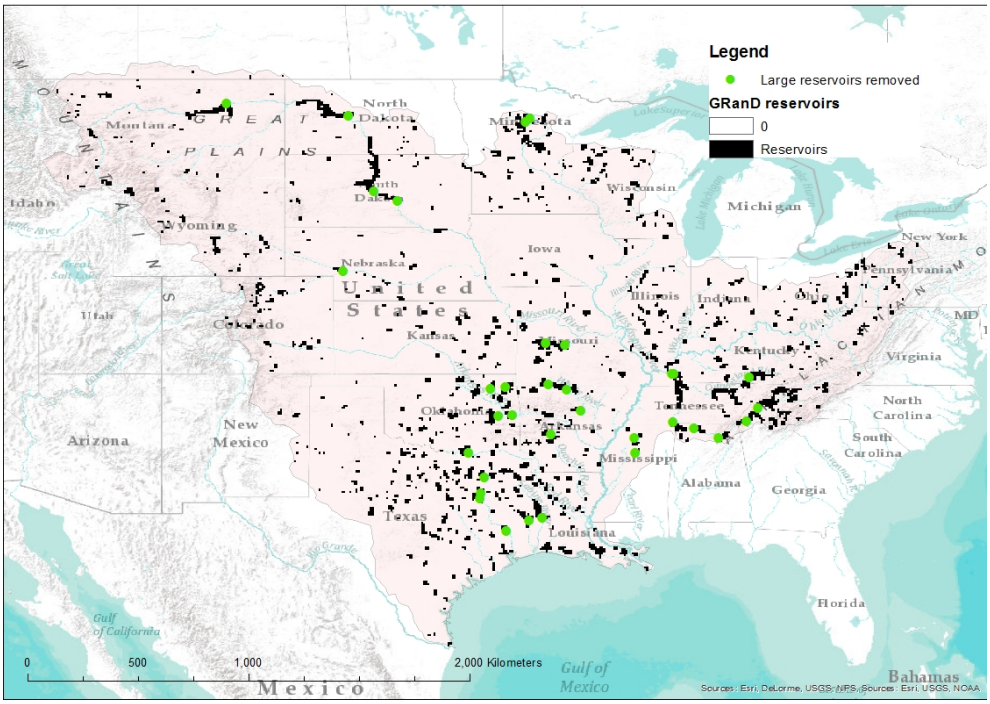

Figure 4.3: Overview map representing the scenario in which the large reservoirs are removed.

4.5 Analysis

Figure 4.4: Location of observation points in the Mississippi River basin.

The resolutions and format of the model output is in a NetCDF (*.nc) format (Network Comman Data Form i.e. a set of software libraries and self-describing, machine-independent data formats that support the creation, access and sharing of array-orientated scientific data). The output files contained daily data for the entire modelling period (1980-2014), which was recalculated to monthly sums and averages using the cdo function 'monsum' and 'monmean'. The seasonal, temporal and spatial variability were analyzed at several observation point along the Mississippi and its tributaries (Figure 4.4, Table 4.5). The data at the observation points was extracted from the model output using a python script based on coordinate locations.

Table 4.5: Coordinates, average discharge, drainage area and river name of observation locations.

Location	Coordinates [lon, lat]	Average annual discharge $[m^3/s]$	Drainage Area $[km^2]$	River Name
Clinton	(-90.21 ; 41.79)	920	$2.2 * 10^5$	Upper-Mississippi
Hermann	(-90.79 ; 38.54)	4120	$1.35 * 10^6$	Missouri
Olmsted	(-89.04 ; 37.13)	4610	$5.26 * 10^5$	Ohio River
Tarbert Landing	(-91.63 ; 31.04)	16280	$2.91 * 10^6$	Lower-Mississippi

4.5.1 Analyzing temporal variability

To validate the results of the model the monthly sediment transport was recalculated to the total annual suspended sediment transport. The temporal variability and magnitude of the calculated annual sediment transport (at all observation points for the scenario with all reservoirs) were compared to other studies that describe the annual suspended sediment flux in recent years. Furthermore, the total annual suspended sediment transport at Hermann, Olmsted and Tarbert Landing was analyzed for all scenarios to evaluate the effect of the construction and removal of reservoirs on the year-to-year variability.

The seasonal variability of the model output was analyzed at Tarbert Landing and Hermann for the scenario with and without reservoirs. To this extent the model output was recalculated to average monthly sediment transport and average monthly discharges. The average discharge and monthly sediment transport calculated from the entire modeling period (1980-2014) were compared to the extremely wet year 1993 and the extremely dry year 2012 to evaluate the effect of reservoir construction on the seasonal variability in normal and extreme years.

4.5.2 Analyzing spatial variability

To analyze the spatial differences in sediment transport along the channel for the entire MRB, maps that represent the average annual sediment transport over the entire time period were produced. The total annual sediment transport was calculated using the 'yearsum' function of cdo, which calculates the yearly sum from the monthly sediment transport values generated by PCR-GLOBWB. The yearly sums were averaged using the 'timmean' function of cdo and converted to a single map for each scenario. All produced maps were transferred to ArcMap and reclassified into the same classes.

Maps of the entire MRB were produced for the scenario with and without reservoirs to analyze the spatial differences between the potential and actual sediment transport. The total potential sediment flux was calculated using the 'accuflux' function of PCRaster, which calculates for each cell the accumulated amount of material that flows out of the cell into its neighboring downstream cell, from the LDD and sediment production map (Equation 4.23).

$$\text{Total potential suspended sediment flux} = \text{accuflux}(\text{ldd}, \text{Sediment production map}) \tag{4.23}$$

In which the ldd is a spatial map and the sediment production and total suspended sediment flux are spatial scalars. The accumulated amount therefore represents the amount of material in the cell itself plus the amount of material coming from upstream cells. The actual sediment transport flux was obtained by deriving the monthly average sediment transport data from the PCR-GLOBWB model runs. The ratio between these sediment fluxes was calculated by dividing the actual sediment transport flux by the potential sediment flux. From these calculations, maps were produced of the entire MRB represented in log scale.

4.5.3 Analyzing scenarios

The average annual suspended sediment transport over the entire modeling period was calculated for every observation point and scenario to analyze the effect of the removal of selected reservoirs on the suspended sediment flux. To evaluate the effect of the construction of reservoirs and the removal of selected reservoirs the relative difference between the scenario without reservoirs and the other scenarios was calculated.

Chapter 5

Results

5.1 Calibration and Validation

5.1.1 Calibration

After the first model run, the sediment production per sub-catchment was calibrated to obtain more accurate results in comparison to reported sediment transport values. These adjusted values for the sediment production are added in the last column of Table 5.1. Further calibration was unfortunately beyond the scope and time of this research, although the model output still shows a relatively large error in comparison to other reported values.

Table 5.1: Calibrated sediment production per sub-catchment.

Hydrologic Unit	Sediment Production $[kg/m^2/year]$	Calibrated Sediment Production $[kg/m^2/year]$
Missouri	0.214	1.692
Upper Mississippi	0.067	0.488
Ohio	0.137	0.553
Arkansas / Red / White	0.189	0.895
Lower Mississippi	0.024	0.024

5.1.2 Validating results

Several articles (Keown et al. (1986); Meade and Moody (2010); Heinemann, Sprague and Blevins (2011); Horowitz (2010)) estimated the average annual sediment transport in the Mississippi River and its tributaries before and after the construction of dams and reservoirs. These estimates were based on actual suspended sediment data obtained in the field. An overview of the average annual sediment transport values found in literature, the values found with PCR-GLOBWB and the relative error range between these values is presented in Table 5.2. The largest relative error is found at Clinton with a value of 6.7, unfortunately providing a range of errors was not possible at this location as only Horowitz (2010) reported his finding for the Upper-Mississippi. The relative error is 2.5 on average for both scenarios at Tarbert Landing and for the scenario with all reservoirs at Hermann, an exception is the large relative error of 4 found at Hermann for the scenario without reservoirs. Horowitz (2010) and Heinemann et al. (2011) derived an average annual suspended sediment load at Grand Chain, which can be compared to the values found at Olmsted, as the cities are located only 10 kilometers apart. The relative error is fairly small at this

location if compared to that of Horowitz, but average if compared to the research of Heinemann. Meade and Moody (2010) estimated a decline in sediment transport at Tarbert Landing from approximately 300 MT/y to 110 MT/y (Table 5.2), resulting in a relative decline of 63%. The PCR-GLOBWB model without reservoirs yields an average annual sediment transport at Tarbert Landing of approximately 110 MT/y, which reduces to approximately 42 MT/y if all reservoirs are included. The relative decline at Tarbert Landing is therefore approximately 62%, which is in the same order of magnitude as the decline measured in the research of Meade and Moody.

Table 5.2: Overview of relative error range between values found in literature and the model output of PCR-GLOBWB (blue: Keown et al. (1986); red: Meade and Moody (2010); green: Horowitz (2010); magenta: Heinemann et al. (2011)).

Observation Point	Scenario	Literature	PCR-GLOBWB	Relative error range
Tarbert Landing	No Reservoirs	271 - 300	110	2.5 - 2.7
	All Reservoirs	100 - 110	42	2.4 - 2.6
Hermann	No Reservoirs	289 - 300	71	4.0 - 4.1
	All Reservoirs	55 - 55.8	22	2.5 - 2.54
Clinton	All Reservoirs	3	0.45	6.7
Olmsted	All Reservoirs	28 - 40.3	18	1.6 - 2.4

Horowitz (2010) described the trends in annual suspended sediment transport based on measurements of the USGS. The trends at all observation locations can be compared to the model results at these locations presented in Figure 5.1, 5.2, 5.3 and 5.4. Although the measured values in annual sediment transport in the research of Horowitz are significantly higher, the year-to-year variability shows similar trends as the year-to-year variability in this research until the year 1995. After this year the model shows a steady decline in sediment transport while Horowitz finds a period with increasing values. An exception is the temporal suspended sediment trend found at Olmsted which seems to show a very similar year-to-year variability as Horowitz for the entire period (1980-2008). The trend in the year-to-year variability at Hermann derived by Heinemann et al. (2011) seems to fit the variability found in this research better than the trend found by Horowitz (2010), even after the year 1995. The increase in sediment transport in the period 1995-1999 found by Horowitz is not as profound in the trend derived by Heinemann, although both researches used the same USGS database.

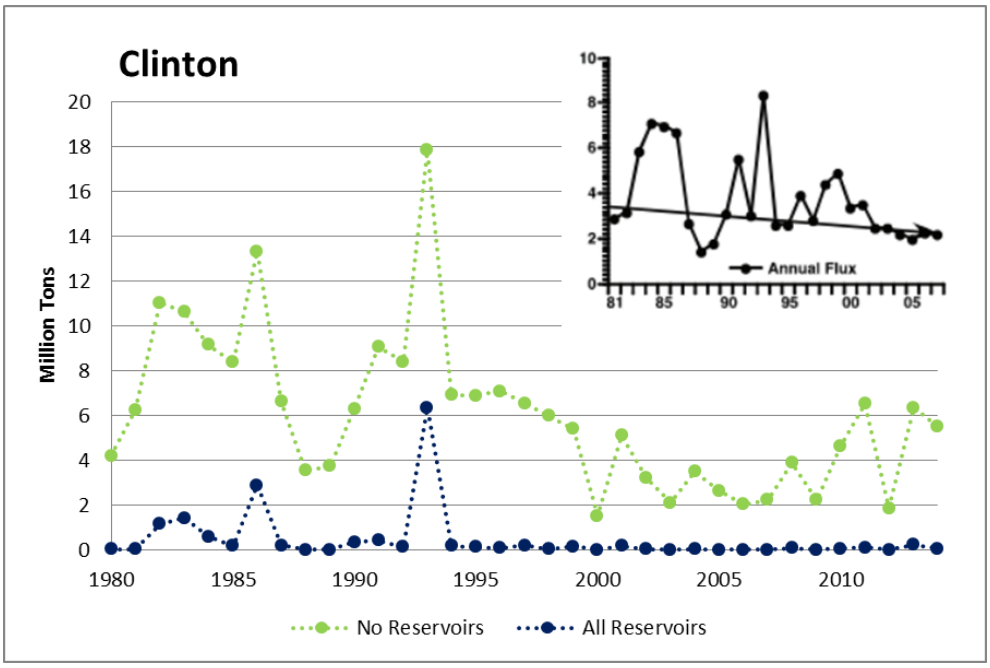

Figure 5.1: Total annual sediment transport at Clinton for the period 1980-2014 derived from the PCR-GLOBWB model and from Horowitz (2010).

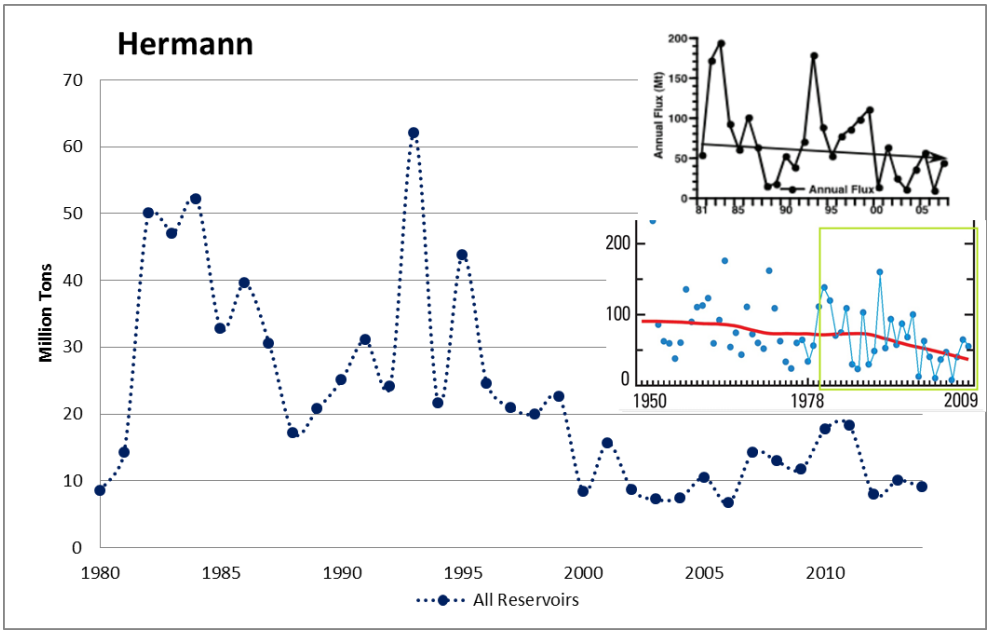

Figure 5.2: Total annual sediment transport at Hermann for the period 1980-2014 derived from the PCR-GLOBWB model, Horowitz (2010) and Heinemann et al. (2011).

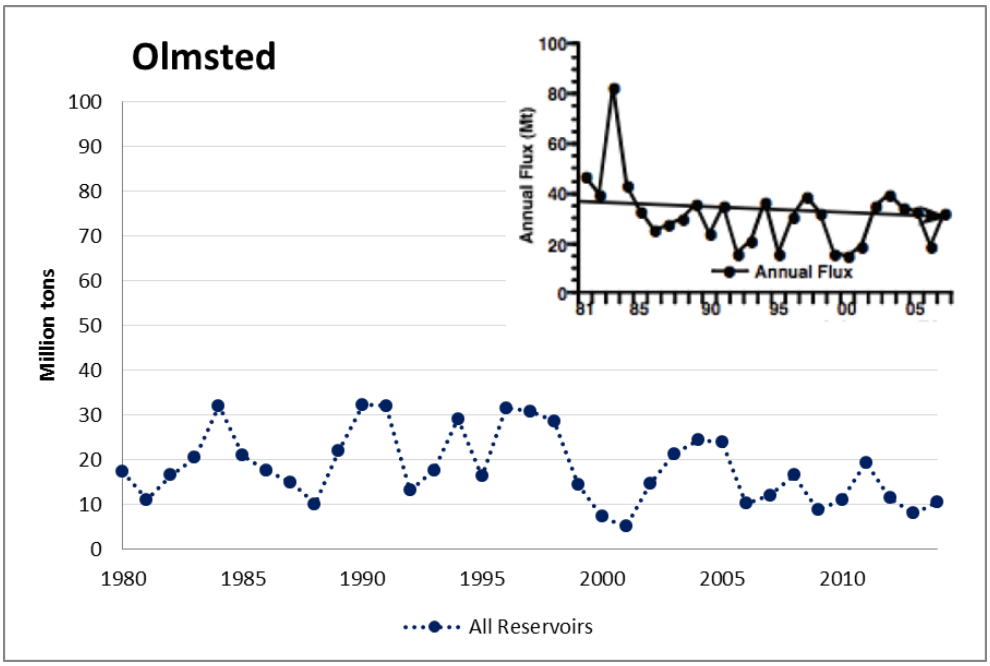

Figure 5.3: Total annual sediment transport at Olmsted for the period 1980-2014 derived from the PCR-GLOBWB model and from Horowitz (2010).

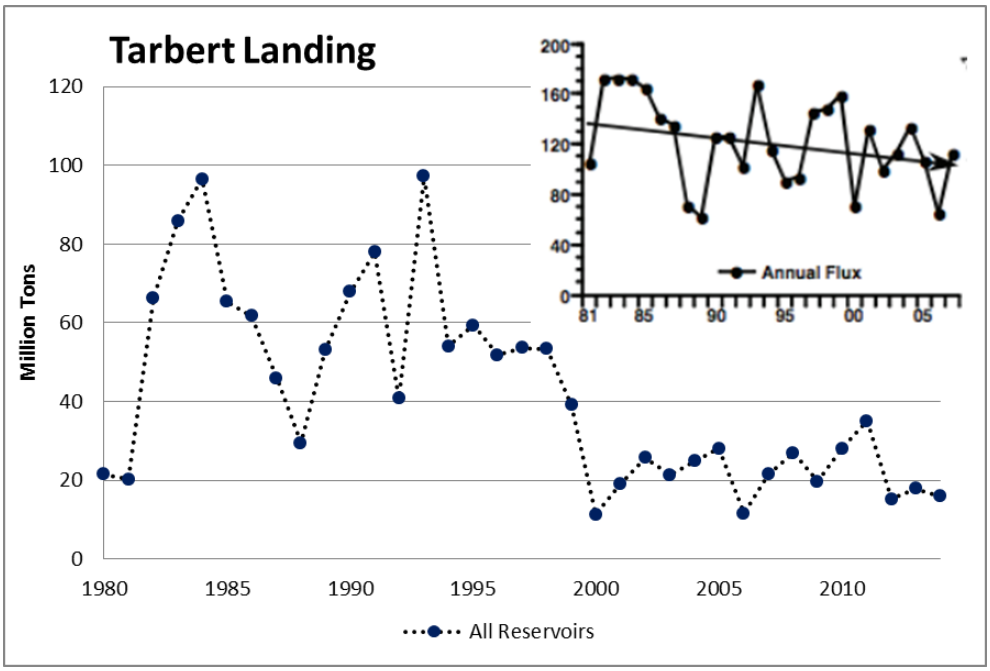

Figure 5.4: Total annual sediment transport at Tarbert Landing for the period 1980-2014 derived from the PCR-GLOBWB model and from Horowitz (2010).

5.2 Temporal variability in sediment transport

5.2.1 Annual variability

Figure 5.5, 5.6 and 5.7 represent the average annual suspended sediment transport for the period 1980-2014 at Hermann, Olmsted and Tarbert Landing for all the scenarios. At all locations the scenario with reservoirs showed considerably less year-to-year variability than the scenario without reservoirs. The extremes are less apparent and of a smaller magnitude and the deviations from the average are minor. At Hermann and Tarbert Landing the year-to-year variability in the sediment transport seems larger in the period 1980-1999 than in the period 1999-2014, this effect can however not be observed at Olmsted. The year-to-year variability in scenarios that include the removal of the Missouri, Ohio or large reservoirs is very variable between the different locations, but always lies in-between the two end member scenarios (no reservoirs or all reservoirs included). The variability at a certain observation point is dependent on the influence of the scenario simulation on the annual average sediment transport, if the effect is small (such as the influence of the removal of the Ohio dams at Tarbert Landing) the year-to-year variability is small and similar to that of the scenario that includes all reservoirs.

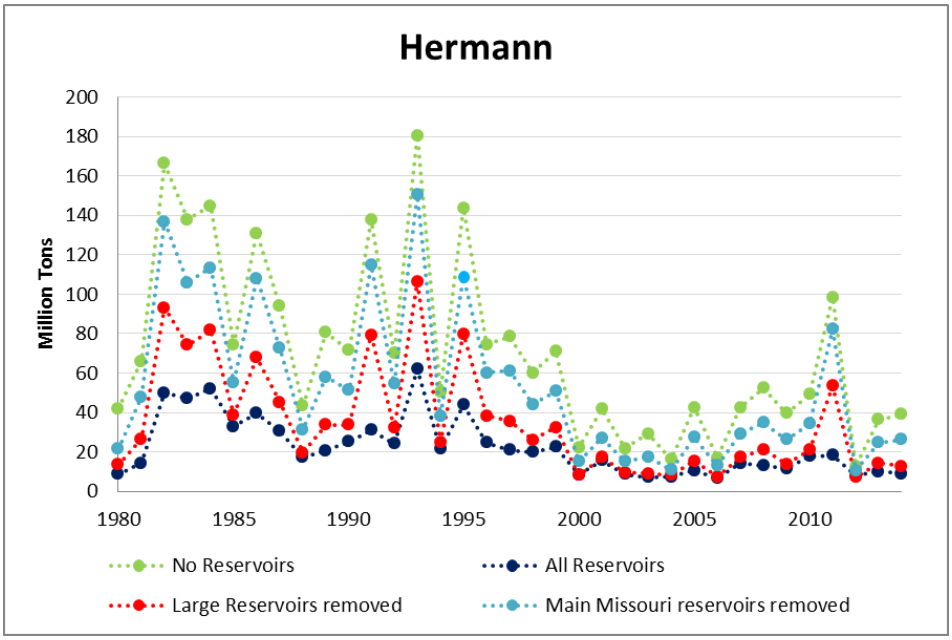

Figure 5.5: Average annual suspended sediment transport for the period 1980-2014 at Herman, Missouri River.

Table 5.3 presents the average, the standard deviation and the coefficient of variation (CV) for the average annual sediment transport and discharge for each observation point and scenario. A small CV means that the data are tightly clustered around the mean, while a large number means that the data are more spread out. In this research, the CV has high values for both the sediment transport and discharge for all observation points and scenarios. This is because both sediment transport and discharge are highly variable over time. Therefore, the CV gives an indication of the dependence on extreme events. For the discharge, the value of CV is fairly constant for all scenarios on a given observation point. This means that although the values of CV may be high, all the scenarios have a similar variability. At Clinton the CV of sediment transport is significantly higher for the scenarios with reservoirs than for the scenario without reservoirs, this probably means that the sediment transport at Clinton is highly influenced by extreme events. This effect

can also be seen in Figure 5.1, which shows extreme maxima in the year 1986 and 1993. For all the other observation points the differences for the CV of sediment transport are not substantial.

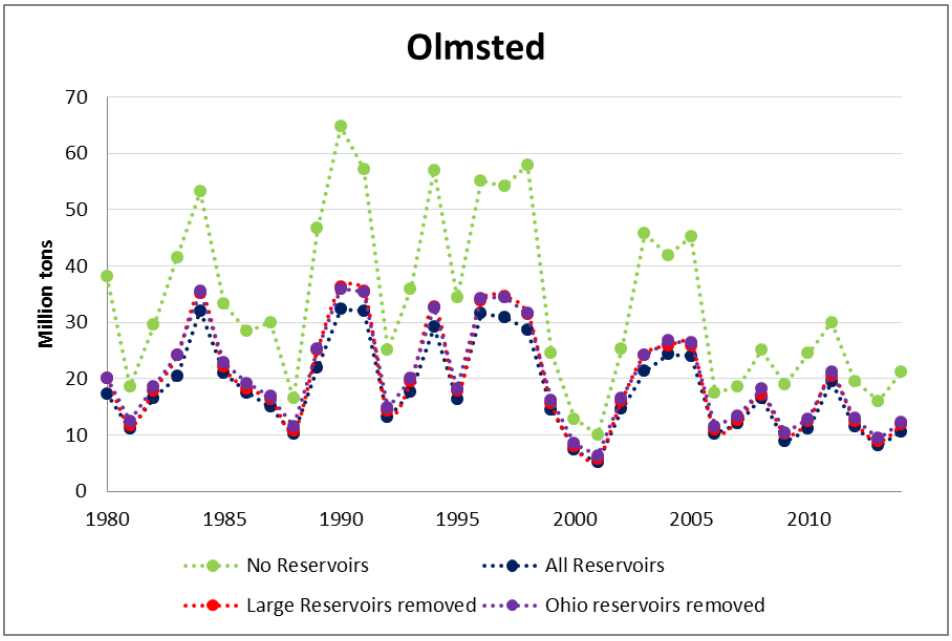

Figure 5.6: Average annual suspended sediment transport for the period 1980-2014 at Olmsted, Ohio River.

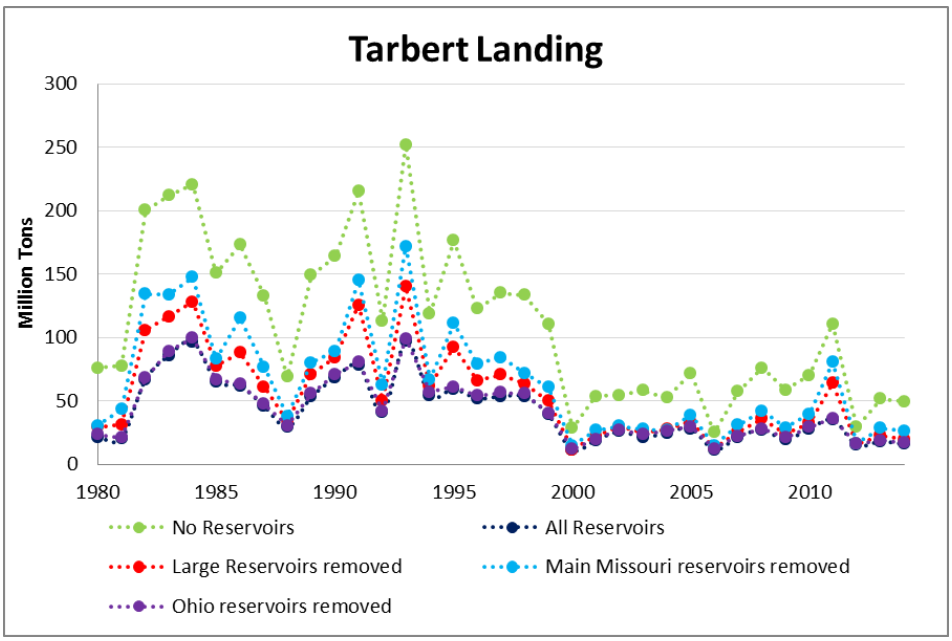

Figure 5.7: Average annual suspended sediment transport for the period 1980-2014 at Tarbert Landing, Lower-Mississippi River.

Table 5.3: Overview of sediment transport and discharge average, standard deviation and coefficient of variation for all observation points and scenarios.

Clinton	Average annual sediment transport (MT/yr)	STD dev	CV	Average discharge (m^3/s)	STD dev	CV
No Reservoirs	6.03	3.51	0.58	916	623	0.68
All Reservoirs	0.45	1.17	2.59	916	623	0.68
Large reservoirs removed	0.46	1.17	2.57	920	626	0.68
Missouri reservoirs removed	0.45	1.17	2.59	916	623	0.68
Ohio reservoirs removed	0.45	1.17	2.59	916	623	0.68
Hermann						
No Reservoirs	71	46	0.64	4117	2497	0.61
All Reservoirs	22	14.6	0.66	4117	2497	0.61
Large reservoirs removed	35	27.5	0.79	4244	2852	0.67
Missouri reservoirs removed	54	38.4	0.72	4207	2810	0.67
Ohio reservoirs removed	22	14.6	0.66	4719	2286	0.48
Olmsted						
No Reservoirs	34	15.2	0.45	5160	2764	0.54
All Reservoirs	18	8.0	0.44	4608	2182	0.47
Large reservoirs removed	19.9	8.9	0.45	4735	2328	0.49
Missouri reservoirs removed	18	8.0	0.44	4608	2182	0.47
Ohio reservoirs removed	20.3	8.7	0.43	4719	2286	0.48
Tarbert Landing						
No Reservoirs	110	62.2	0.57	16284	7596	0.47
All Reservoirs	42	24.5	0.59	16284	7596	0.47
Large reservoirs removed	56	36.0	0.65	16641	8197	0.49
Missouri reservoirs removed	66	43.2	0.66	16375	7897	0.48
Ohio reservoirs removed	44	25.0	0.58	16395	7677	0.47

5.2.2 Seasonal variability

This section describes the differences in seasonal variability for the scenario with and without reservoirs at Hermann (Figure 5.8) and Tarbert Landing (Figure 5.9). The average discharge and sediment transport were compared to the extremely wet year 1993 and the extremely dry year 2012 to analyze the seasonal variability for normal and extreme years. An overview of the relative decline in annual average discharge and sediment transport between the scenario with and without reservoirs is presented in Table 5.4 and 5.5 and the occurrence of peak discharges and maxima in sediment transport is summarized in Table 5.6 .

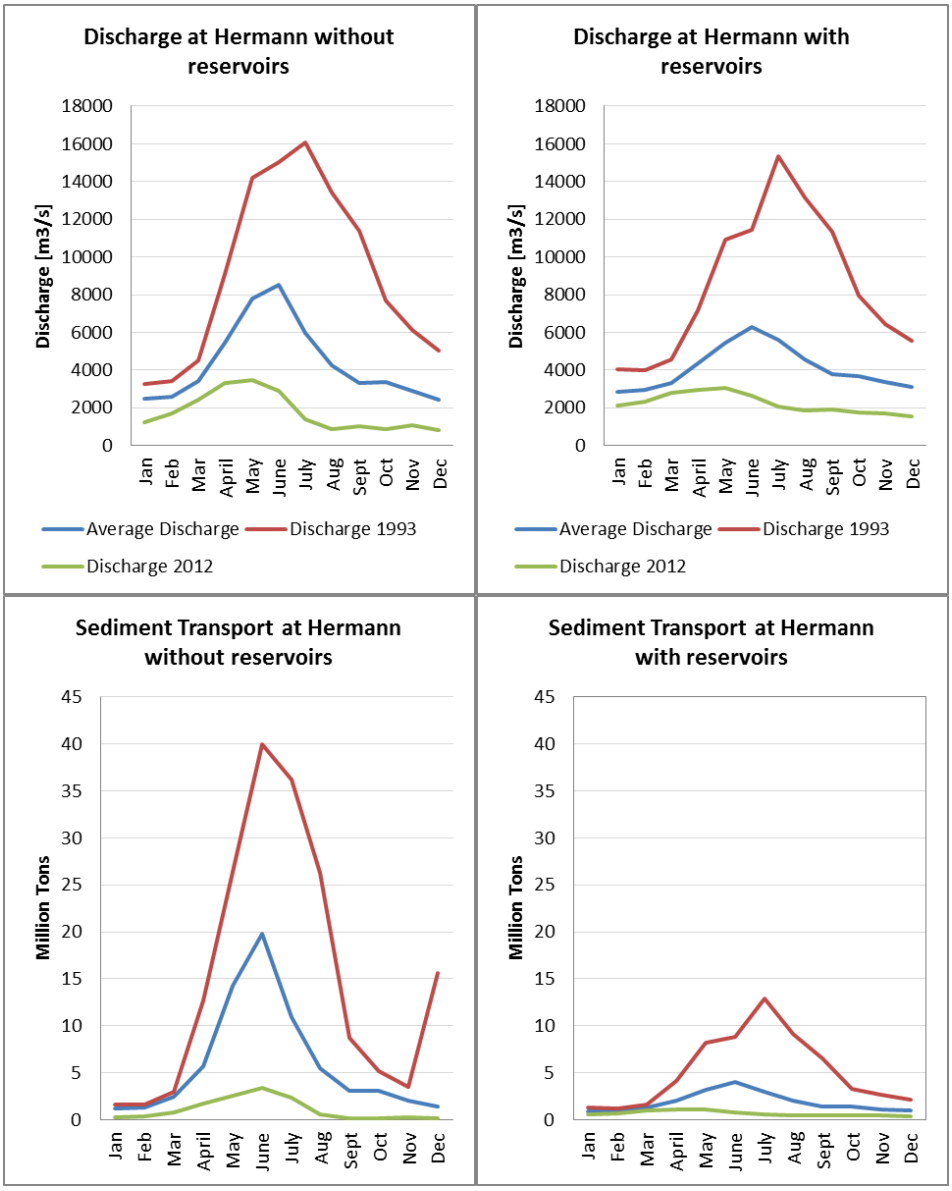

Figure 5.8: Overview of discharge and sediment transport per month at Hermann.

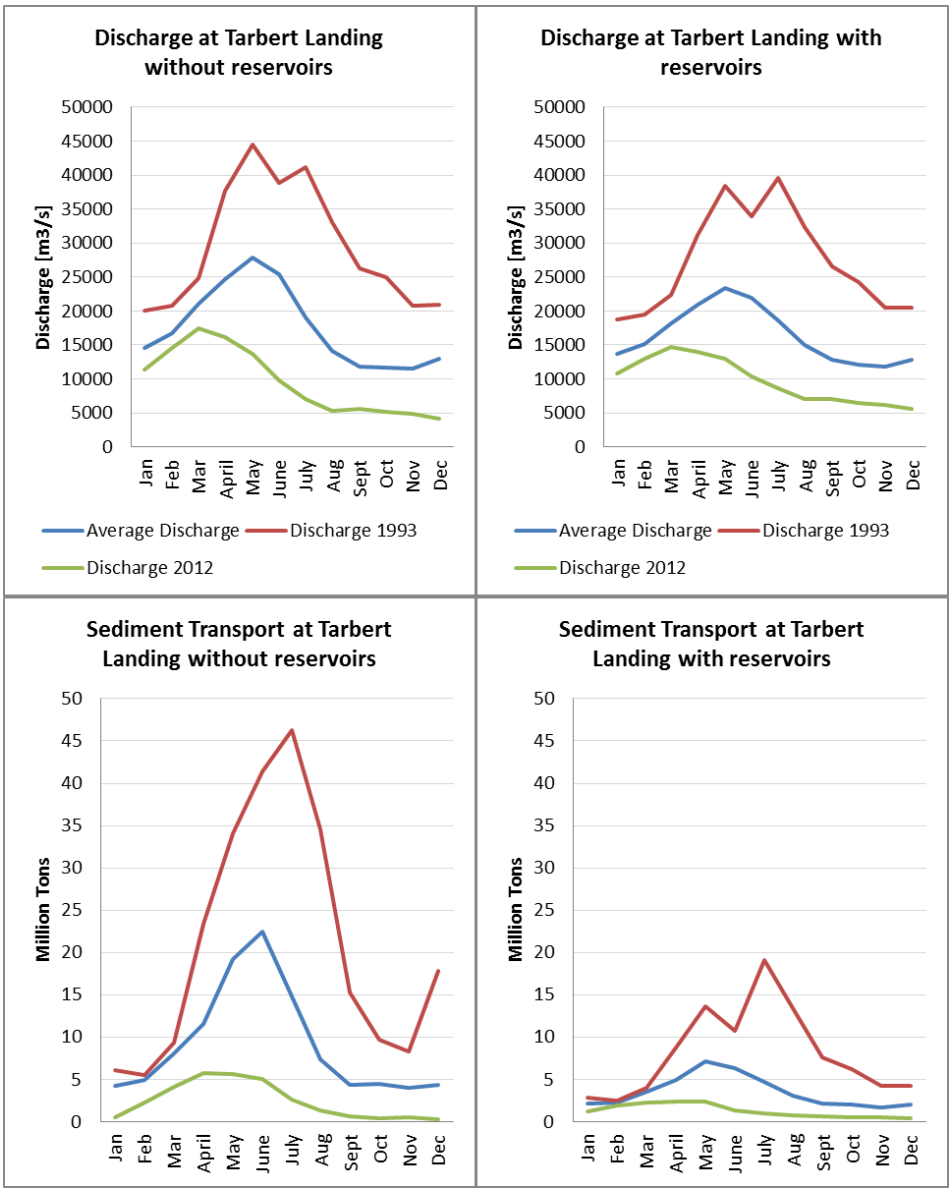

Figure 5.9: Overview of discharge and sediment transport per month at Tarbert Landing.

Table 5.4: Overview of relative decline in average discharge for the average year, 1993 and 2012.

Average discharge $[m^3/s]$				
		No Reservoirs	All Reservoirs	Relative Difference
Hermann	Average year	4374	4111	-6.0
	Year 1993	9108	8491	-6.8
	Year 2012	1752	2228	27.1
		No Reservoirs	All Reservoirs	Relative Difference
Tarbert Landing	Average year	17635	16353	-7.3
	Year 1993	29498	27330	-7.3
	Year 2012	9595	9711	1.2

Table 5.5: Overview of relative decline in annual sediment transport for the average year, 1993 and 2012.

Average annual sediment transport $[MT/yr]$				
		No Reservoirs	All Reservoirs	Relative Difference
Hermann	Average year	70.6	22.1	-68.6
	Year 1993	180.6	62.0	-65.7
	Year 2012	12.7	7.9	-37.6
		No Reservoirs	All Reservoirs	Relative Difference
Tarbert Landing	Average year	109.9	41.8	-61.9
	Year 1993	251.7	97.2	-61.4
	Year 2012	29.1	15.2	-47.8

Table 5.6: Occurrence of peak discharges and maxima in sediment transport

Hermann			
Scenario	Year	Peak discharge	Maximum sediment transport
No reservoirs	Average year	June	June
	Year 1993	July	June
	Year 2012	May	June
All reservoirs	Average year	June	June
	Year 1993	July	July
	Year 2012	May	April
Tarbert Landing			
Scenario	Year	Peak discharge	Maximum sediment transport
Without reservoirs	Average year	May	May
	Year 1993	May	June
	Year 2012	March	March
With reservoirs	Average year	June	May
	Year 1993	July	July
	Year 2012	April	May

At both locations, the discharge showed a smaller range with lower maximum values and fewer extremes for the scenario with reservoirs than for the scenario without reservoirs. This effect can be observed more clearly for the average year and the year 2012 than for the year 1993. The extremely wet year 1993 and the average year show a relative decline in average annual discharge that ranges between -6 and -7.3% (Table 5.4). The year 2012, however shows a relative increase in annual average discharge of 27.2% at Hermann to 1.2% at Tarbert Landing. The relative increase in discharge for the year 2012 is primarily caused by the regulating effect of reservoirs, which increases the minimum discharge and lowers the maximum discharge. The sediment transport showed a significant decline if the reservoirs were introduced, as the reservoirs do not only alter the seasonal variability but also the magnitude due to trapping. The year 1993 and the average year show a similar relative decline in annual sediment load (-62% and -61% respectively at Tarbert Landing), while the year 2012 shows a much smaller decline (-48% at Tarbert Landing) (Table 5.5). This smaller decline is likely caused by the higher annual average discharge that occurs if the reservoirs are included. The storage capacity of the reservoirs delays the response of the discharge dynamics to extreme events. In most years this effect can be observed as a delay in occurrence of the peak discharge and maximum sediment transport (Table 5.6).

5.3 Spatial variation in sediment transport

5.3.1 Sediment transport along the channel

The maps represented in Figure 5.10 and 5.11 show the average annual sediment transport [in MT/yr] over the period 1980-2014 for all the scenarios. From these maps the differences in sediment transport along the channel for all the scenarios can be analyzed. As expected, the map for the scenario without reservoirs shows the highest values in sediment transport and the most distinct river system. The sediment transport along the channel changes gradually from low values in the tributaries, to intermediate values in the rivers and high values in the Missouri and Lower Mississippi. When the reservoirs are included, the sediment transport over the entire river system reduces and the river channel is interrupted by reservoirs (grey polygons). As mentioned before, sediment that passes through a reservoir is set to the outflow point. Therefore sediment transport in the reservoirs is not quantified in the maps. Similar to the scenario with reservoirs, the main channel of the Lower-Mississippi shows the highest values in sediment transport. The main channel of the Missouri shows however a significant decline in sediment transport. Although many differences can be seen along the main channel of the Missouri, the Upper-Missouri and most of the tributaries do not show an extreme decline in sediment transport. The scenario that includes the removal of the main Missouri River dams shows the highest annual sediment transport in comparison to the scenarios that include the removal of the Ohio and large reservoirs. The removal of the Ohio reservoirs, results in a map that is similar to the map representing the removal of all reservoirs, which is not remarkable taking into account the the relatively small percentage of reservoir capacity that was removed in this scenario. All maps show similar values for the sediment transport in the tributaries, although the simulated transport is slightly higher for the scenario without reservoirs.

To quantify the contribution of the tributaries to the sediment transport, a comparison was made between the actual and potential sediment transport upstream and downstream of the Missouri and Ohio River. The downstream observation points were Hermann (Missouri) and Olmsted (Ohio), while the upstream observation points were chosen based on the transition point between streamorder 5 and 6 (Figure 5.12). Table 5.7 represents an overview of the ratio between the actual and potential sediment flux at the chosen observation points. The ratio declines at all observation points if the reservoirs are included, as a result of the reduction in sediment transport. Furthermore, the ratio is higher at the upstream observation points than at the downstream observation point.

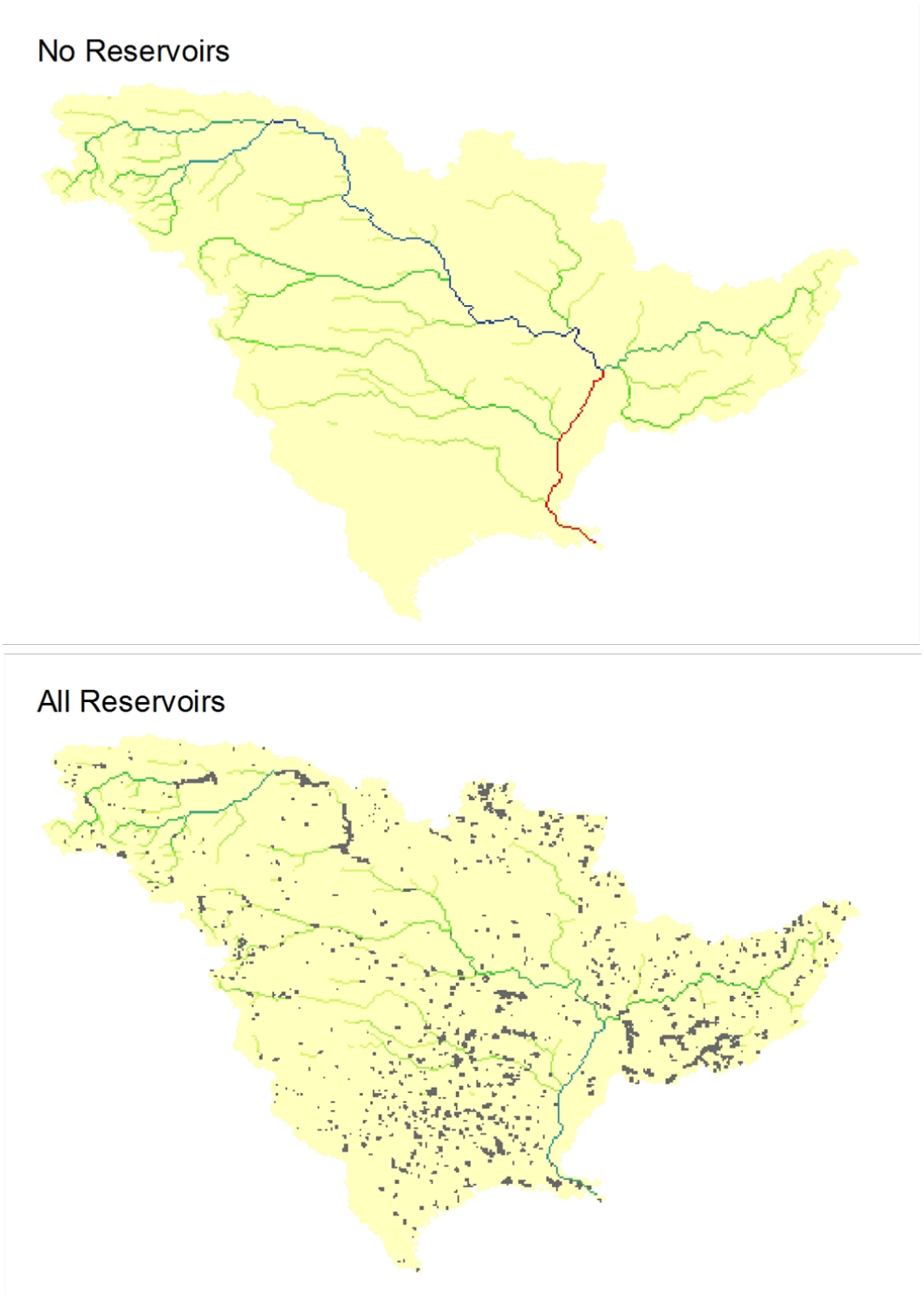

Figure 5.10: Average annual sediment transport for the all catchments in the MRB in [MT/yr].

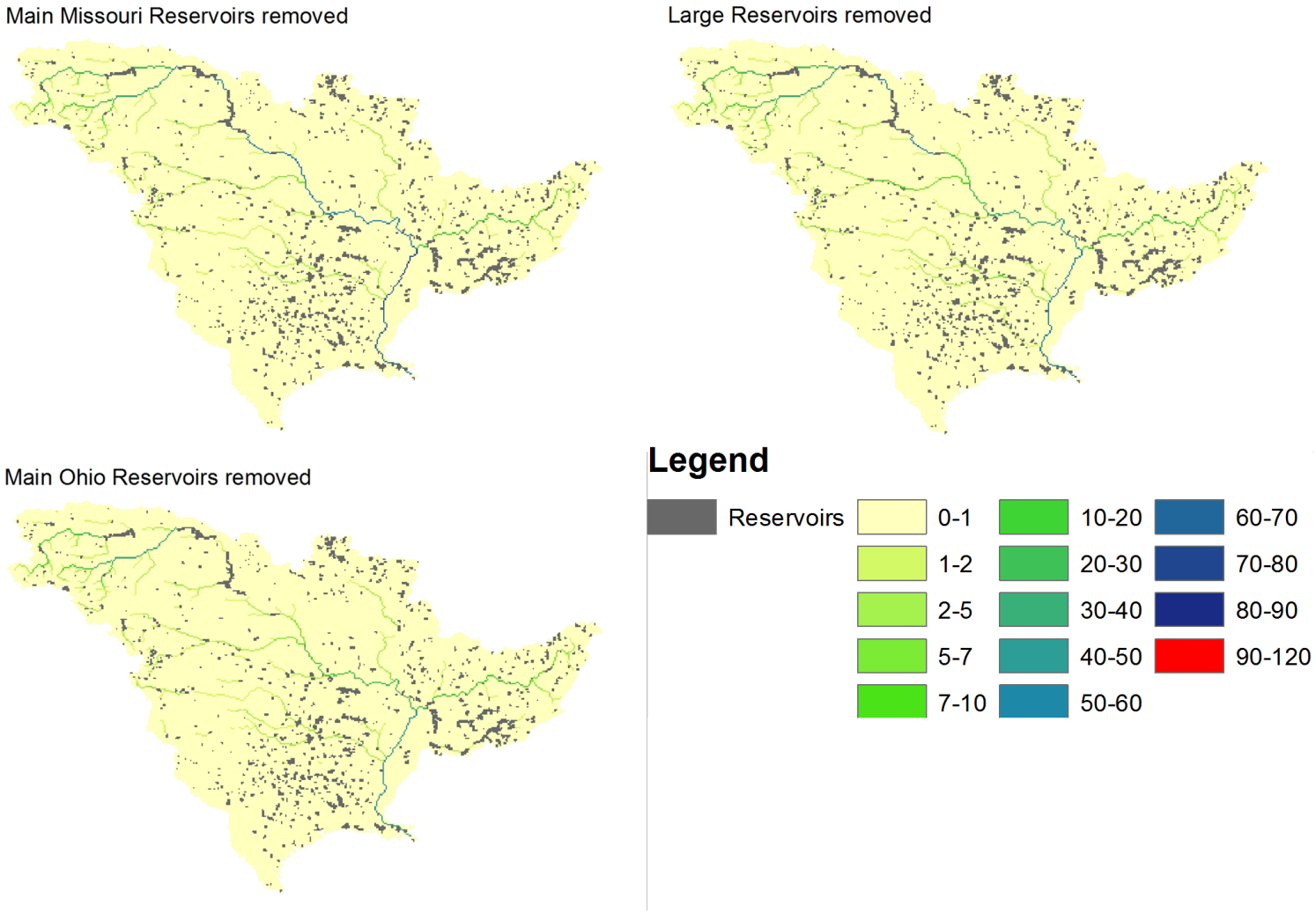

Figure 5.11: Average annual sediment transport for the all catchments in the MRB in [MT/yr].

Table 5.7: Overview of the relative difference between the potential and actual sediment flux at an upstream and downstream location along the Missouri and Ohio River.

		Potential Sediment Flux [MT/yr]	Actual Sediment Transport [MT/yr]		Actual/Potential	
			No Reservoirs	All Reservoirs	No Reservoirs	All Reservoirs
Missouri	Upstream	225	27	19.5	0.142	0.104
	Downstream (Hermann)	2258	71	22	0.031	0.0097
		Potential Sediment Flux [MT/yr]	Actual Sediment Transport [MT/yr]		Actual/Potential	
			No Reservoirs	All Reservoirs	No Reservoirs	All Reservoirs
Ohio	Upstream	27.4	8.3	5.7	0.303	0.208
	Downstream (Olmsted)	291	34	18	0.117	0.062

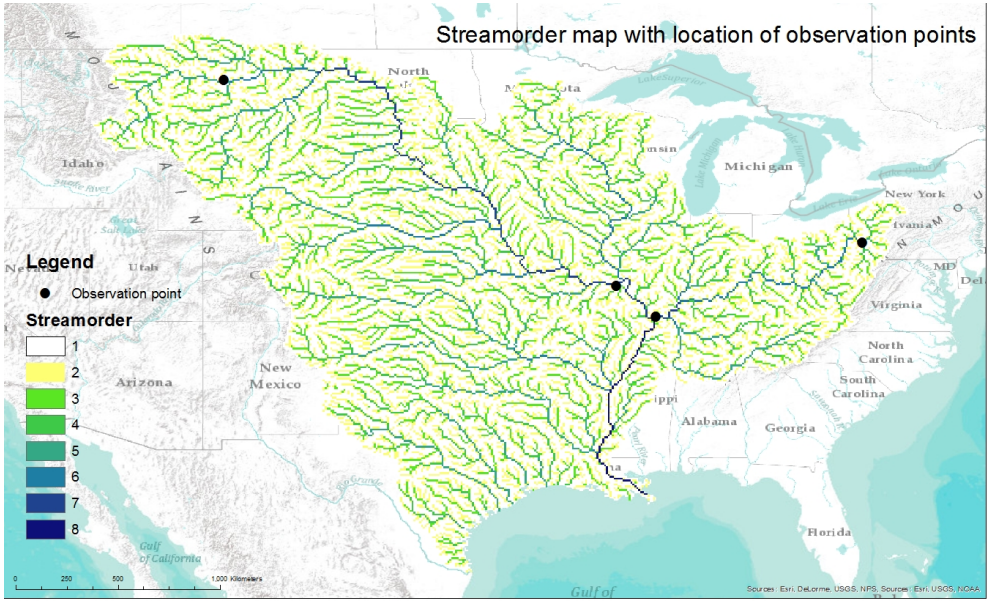

Figure 5.12: Overview of streamorder network with observation points for Table 5.7.

5.3.2 Comparing actual sediment transport to the potential sediment transport

The maps presented in Figure 5.13 show the log of the ratio between the actual sediment transport and the potential sediment transport for the entire MRB and the Missouri catchment for the scenario with and without reservoirs. In these maps, a value approaching one (or in map $log(1) = 0$) indicates that all sediment present in the area upstream of a cell is mobilized and transported downstream, while lower values indicate a decline in mobilization and transportation. For example, the Great Plains in the Missouri catchment are for both scenarios approaching a value of one. This means that all sediment already present in the cell and the amount of sediment in the upstream cells of the cell is transported downstream. When comparing the maps of the different scenarios, it becomes apparent that more of the available sediment is routed downstream in the scenario without reservoirs than in the scenario with reservoirs. The reservoirs (grey polygons) appear as 'gaps' in the river when they are included in the model. This is because (Section 4.2) all sediment load located in the water bodies is set to the outflow point.

5.4 Scenarios

Figure 5.14 presents the average annual sediment transport in MT/yr for the period 1980-2014 for each scenario and observation point and Figure 5.15 presents the relative decline in the annual average sediment transport between the scenario without reservoirs and the other scenarios for each observation point. The decline in annual average is largest at Clinton, which is remarkable as previous researches do not describe a significant decline in sediment transport in the Upper-Mississippi catchment (e.g. Keown et al. (1986), Heinemann et al. (2011). The relative decline at Clinton is fairly constant for all scenarios, as none of the simulated scenarios influences the Upper-Mississippi catchment. The scenario that includes the removal of the large reservoirs incorporates two reservoir located in the Upper-Mississippi catchment. The removal of these reservoirs seems to have little effect on the suspended sediment transport at Clinton. The decline in sediment at Clinton is therefore most likely caused by sediment trapping in the large number of small reservoirs. At Herman the relative decline in sediment transport is smaller than at Clinton, the actual decline between the scenario with and without reservoirs of approximately 49 MT/yr is however much larger. The scenario that includes the removal of the Missouri River dams yields the smallest decline in sediment transport resulting in an annual average of 54 MT/yr. The removal of the Ohio reservoirs does not influence the sediment transport in the Missouri and therefore yield the same result as the removal of all reservoirs. At Olmsted the sediment transport declines approximately 46% from an average annual transport of 34 MT/y without reservoirs to 18 MT/y if all reservoirs are included. The removal of the large reservoirs includes 5 of the 9 dams that are removed in the Ohio scenario, which accounts for 91% of the removed reservoir capacity. The annual average sediment transport and relative decline is therefore very similar for these scenarios, although the average annual sediment transport for the removal of the Ohio reservoirs is slightly higher than the average for the removal of the large reservoirs. At Tarbert Landing the average annual sediment transport declines from 110 MT/y for the scenario without reservoirs to 42 MT/y if all reservoirs are included resulting in a relative decline of approximately 62%. The removal of the Missouri reservoirs yields the smallest relative decline of approximately 40.3% to an average annual transport of 66 MT/y. The removal of the large reservoirs results in a relative decline of 49.3%, while the removal of the Ohio reservoirs results in a decline of 60.5%. The removal of the Ohio reservoirs does not have much effect on the sediment transport at Tarbert Landing, this could be expected as only 4.6% of the total reservoir capacity is removed in this scenario (Table 4.4, methods). A remarkable result is that the removal of the Missouri reservoirs yields more sediment transport than the removal of the large reservoirs, as only 26.2% of the total reservoir capacity is excluded for the Missouri scenario against 56.8% for the large reservoirs scenario.

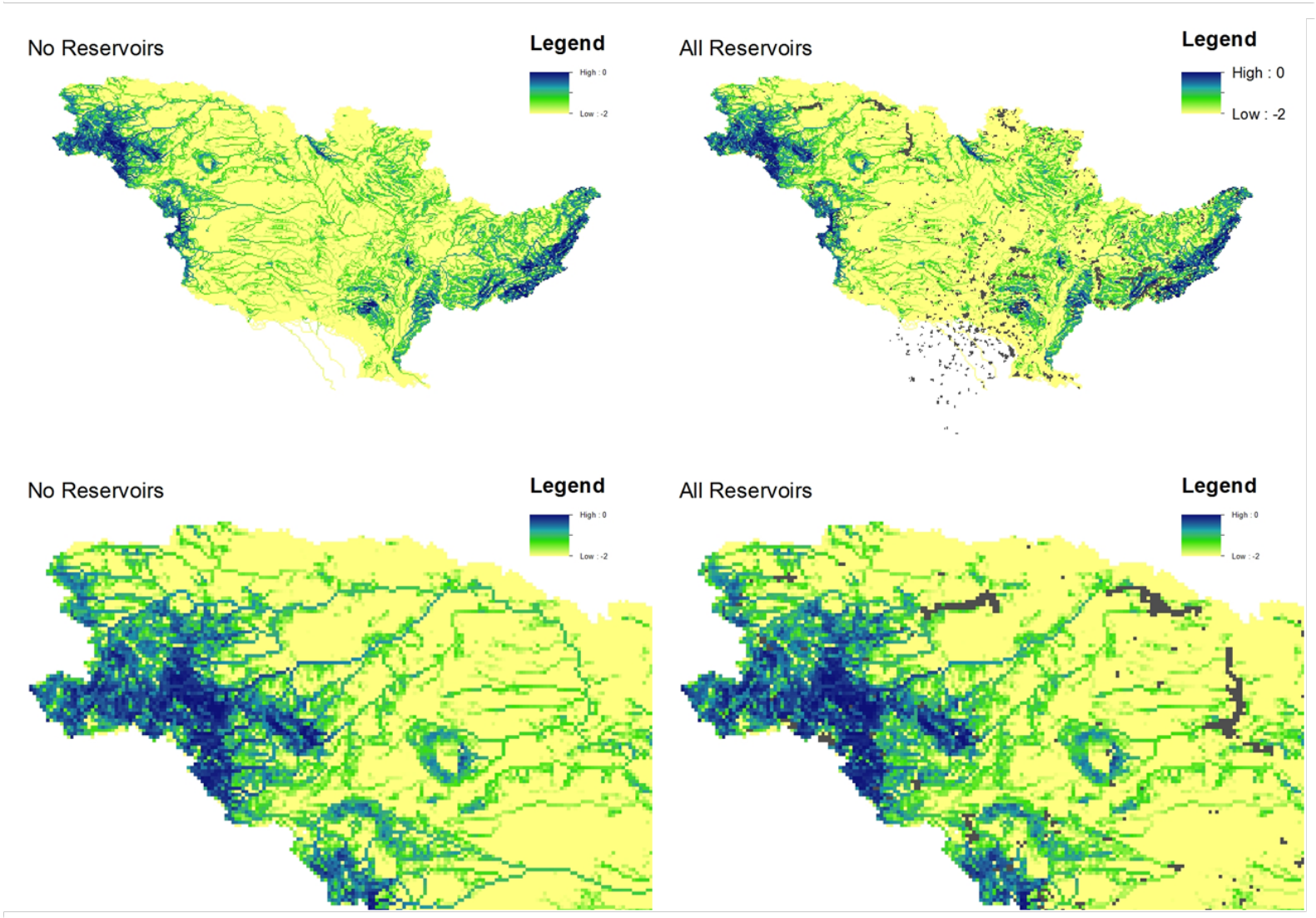

Figure 5.13: Actual sediment transport/potential sediment transport flux for the entire MRB in log-scale.

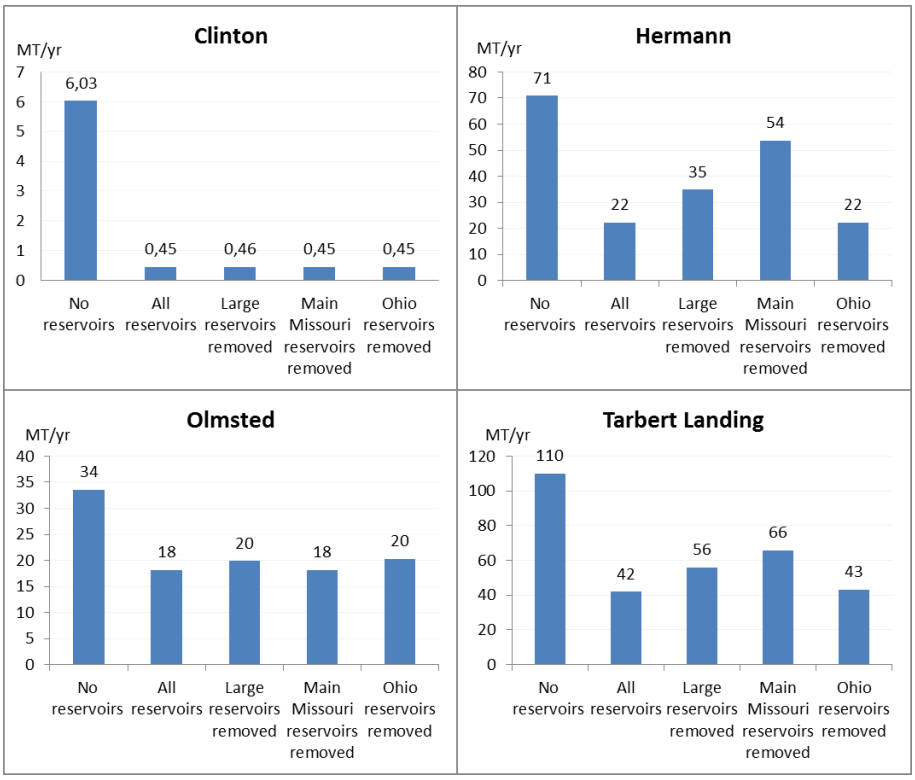

Figure 5.14: Average annual sediment transport [Mt/yr] for each scenario at four observation points along the Mississippi River.

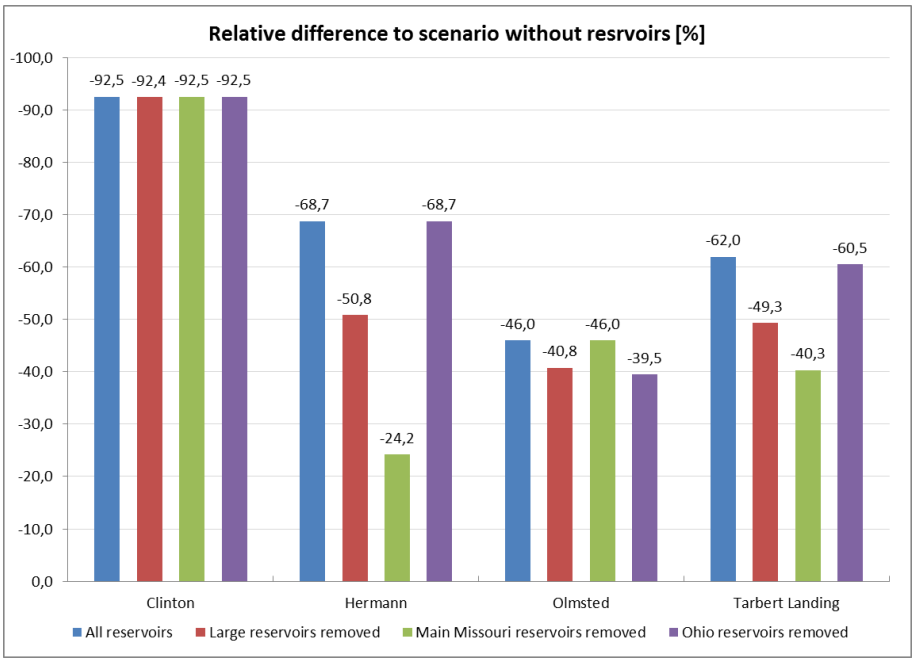

Figure 5.15: Relative decline between the scenario without reservoirs and the other scenarios at each observation point.

Chapter 6

Discussion

6.1 Model performance

The relative error between the reported annual sediment transport and the simulated sediment transport obtained from PCR-GLOBWB are summarized in Table 5.2. The largest relative error was found at Clinton, which can either be caused by an underestimation of the sediment production in the Upper-Mississippi catchment or by the accuracy of the annual mean found by Horowitz (2010), which reported a relatively large error at this location due to the lack of data. The relative error between the literature and the simulation is primarily caused by the sediment production that was used in the PCR-GLOBWB model. Although the sediment production per catchment was based on the natural conditions before human interference, the simulated sediment production without reservoirs is still much lower than in reality. The results of the first model runs were used to calibrate the sediment production to obtain higher values in the simulated sediment transport. Although the sediment production was increased from an average of 0.126 $kg/m^2/day$ to 0.730 $kg/m^2/day$ (345 to 2000 $kg/km^2/day$), the sediment transport is still underestimated by the model. Unfortunately, further calibration was beyond the time of this research.

In this study, the sediment production was assumed to be constant over time for an entire sub-catchment. In reality, extreme precipitation, land use and other natural events result in sudden changes in local erosion, sediment production and delivery, which is not accounted for in the model. Furthermore, the model does not make a distinction between different types of sediment erosion. As a result of this assumption the model does not incorporate local differences in erosion and production and neglects the contribution of bank erosion. Bank incision is enhanced if the discharge is high and the sediment concentration is low (directly downstream of a reservoir), but the model does not account for this process. The suspended sediment transport can therefore easily be underestimated as bank erosion can account for as much as 80% of the total sediment production (Loos, Middelkoop, van der Perk & van Beek, n.d.). According to the results of Kesel (2003) (Figure 2.12) bank calving accounted for as much as 60 MT/yr (assuming $\rho = 1000kg/m^3$) in the period between 1965 and 1972 at the Old River diversion (which is upstream of Tarbert Landing). The model can therefore significantly improve if the process of bank erosion can be included in more detail, if local differences in sediment production are incorporated and if the sediment production is made variable over time.

The year-to-year variability in the simulated annual suspended sediment transport shows a similar interannual variability as the annual sediment transport described by Horowitz (2010) and Heinemann et al. (2011). Therefore, the conclusion can be drawn that the variability in sediment transport in the Mississippi is mainly influenced by changes in hydrologic conditions, which are presented adequately by PCR-GLOBWB. Although the simulated sediment transport shows too

low quantities the interannual variability in the simulated sediment transport is similar to reality.

Blum and Roberts (2009) described different future scenarios for land loss in the Mississippi delta. Their research stated that if the sediment load increases to pre-human conditions (400-500 MT/yr) and the sea-level rises approximately 1 mm/yr no further land loss would occur. If the error factor of 2.4 is taken into account for the scenario without reservoirs, this would result in an average yearly sediment transport of approximately 264 MT/yr. Even in the unlikely scenario that all reservoirs and dams are removed the sediment transport is not sufficient to counteract the effect of relative sea-level rise.

6.2 Temporal variability

6.2.1 Annual variability

At Clinton, Hermann and Tarbert Landing the average annual sediment transport shows considerably less year-to-year variability in the scenarios that include reservoirs than in the scenario without reservoirs (Figure 5.1, 5.2 and 5.4). This decline in year-to-year variability is caused by the regulating and trapping effect of the reservoirs, which reduces the effect of extreme years on the discharge and sediment transport. Furthermore, the year-to-year variability in average annual sediment transport at Clinton, Hermann and Tarbert Landing is larger for the period between 1980 and 2000 than for the period between 2000 and 2014. This lower variability in the period between 2000 and 2014 is the result of a decline in year-to-year variability in the discharge that occurred in this period. Other research (Heinemann et al. (2011); Meade and Moody (2010)) shows a similar decline in year-to-year sediment variability. At Olmsted (Ohio River) the decline in year-to-year variability between the scenario with and without reservoirs is not significant (Figure 5.3). The average annual sediment transport at Olmsted is fairly constant over time and does not show an exceptionally high maximum for the extremely wet year 1993. This constant trend in sediment transport could be because the reservoirs on the Ohio River have a less regulating effect than the reservoirs on the Missouri or by the fairly constant discharge that occurs at Olmsted, which shows fewer extremes than the discharge at the other observation points. This fairly constant trend in long-term discharge pattern and year-to-year variability in the suspended sediment transport of the Ohio River was also noticed in the research of Horowitz (2010).

6.2.2 Seasonal variability

The seasonal variability in the discharge declines significantly if the reservoirs are included (Figure 5.8 and 5.9). The discharge shows a relative decline for the average year and the year 1993 and a relative increase for the year 2012 if the reservoirs are introduced (Table 5.4). The lower seasonal variability is caused by the storage capacity of the reservoirs, which lowers and delays the maximum discharge and increases the minimum discharge. The more constant discharge is one of the most important attributes for reservoir and dam construction, as it enhances the possibility for navigation, transportation, water supply and hydro-power. Furthermore, the peak discharge is delayed by the reservoirs as the storage capacity of the reservoirs is filled before the river water can flow downstream (Table 5.6). In extremely dry years (such as 2012) the reservoir storage can therefore be used to increase the discharge to sustain the transportation and navigation routes, while in extremely wet years the excess water is stored to decrease the river discharge. At both locations, the suspended sediment transport declines in both magnitude and seasonal variability if the reservoirs are introduced. The relative decline in suspended sediment transport is in the same order of magnitude for the average year and the year 1993 (Table 5.5). For the year 2012 the relative decline is less significant at both Hermann and Tarbert Landing, which is probably caused by the increase in discharge that was observed in this year.

The decline in year-to-year variability (described in the previous section) for the scenarios that include reservoirs is probably caused by the decline in seasonal variability. Furthermore, the variability between the scenarios in a certain year (scenario variability) is larger for extremely wet years (such as 1982, 1983, 1991 and 1993) than for extremely dry years (such as 2000, 2006 and 2012). These differences in scenario variability can be observed at all observation points and are the result of the larger seasonal variability that occurs in extremely wet years and the smaller seasonal variability that occurs in dry years.

6.3 Spatial variability

The sediment transport along Mississippi River declines significantly if the reservoirs are introduced (Figure 5.10 and 5.11). The greatest decline can be seen along the main channel of the Missouri and the Lower-Mississippi River. This large decline in suspended sediment transport along the Missouri an Lower-Mississippi was also observed by many other researches (e.g. Heinemann et al. (2011); Kesel (2003); Meade and Moody (2010); Mossa (1996)). The decline in sediment transport along the tributaries is small in comparison to the decline in the rivers and main channels. Therefore, the reservoirs located in the main channel probably have a greater trapping efficiency than the reservoirs located in the tributaries and Upper Missouri. The map representing the removal of the main Missouri reservoirs supports this presumption, as this scenario results in higher sediment transport values along the main channel of the Missouri and the Upper-Mississippi.

The difference between the actual and potential sediment transport declines between the upstream and downstream part of the Missouri and Ohio River (Table 5.13). This indicates that the contribution of the tributaries to the main channel is significant. Whereas a decline between the upstream and downstream point would have indicated that the sediment transport in the tributaries is limited by the transport capacity and the contribution to the main channel is minor. Furthermore, both in the upstream and downstream part the difference between the actual and potential transport declines if the reservoirs are introduced as a result of sediment trapping.

The Great Plains appear to be one of the most prominent sediment sources from which most of the available sediment is routed downstream (Figure 5.13). The contribution of the Great Plains to the river system seems to be independent of reservoir construction. However, in the scenario without reservoirs, more of the available sediment is routed downstream in comparison to the scenario with reservoirs. This reduction in sediment transport downstream, is the result of sediment trapping in the reservoirs which declines the actual sediment transport of the river system.

6.4 Scenarios

An overview of the effects of the different scenarios on the suspended sediment transport at Tarbert Landing are summarized in Table 6.1 (development of scenarios can be found in Section 4.4 and the results per observation point can be found in Figure 5.14 and 5.15 of Section 5.4).

The introduction of reservoirs particularly affected the sediment transport from the Missouri to the Lower Mississippi, which reduced with 68.7% at Hermann and 62% at Tarbert Landing if the reservoirs were introduced. The scenario in which eight main stem Missouri reservoirs were removed resulted in the smallest relative decline in comparison to the scenario without reservoirs, with a relative decline of only 24.2% at Hermann (Missouri River) and 40.3% at Tarbert Landing. The scenario in which 34 large reservoirs were removed had not as much effect on the sediment transport as the removal of the Missouri reservoirs, resulting in a relative decline of 49.3% at Tarbert Landing. Thus, the conclusion can be drawn that although the exclusion of the large reservoirs removes more than twice as much reservoir capacity as the scenario that excludes the main stem Missouri reservoirs, the effects on the sediment transport at Tarbert Landing are minor.

Table 6.1: Summary of the effects of the different scenarios on the average annual suspended sediment transport at Tarbert Landing.

Tarbert Landing				
Scenario	Number of Reservoirs removed	Percentage of reservoir capacity removed	Average annual suspended sediment transport [MT/yr]	Relative decline to scenario without reservoirs
No Reservoirs	713 [all]	-100%	110	0%
All Reservoirs	0 [none]	0%	42	-62%
Large reservoirs removed	34	-57%	56	-49.3%
Main Missouri reservoirs removed	9	-26%	66	-40.3%
Main Ohio reservoirs removed	9	-4.6%	43	-60.5%

This conclusion is remarkable, as the scenario that removes the large reservoirs includes four of the nine removed reservoirs of the Missouri scenario (Appendix B). The scenario in which the nine main stem Ohio reservoirs were removed had a negligible effect on the sediment transport at Tarbert Landing resulting in a relative decline of 60.5% against 62% if all reservoirs are included. This result is in agreement with several other researches that state that the contribution of the Ohio River to the total sediment load at Tarbert Landing is minor in comparison with the western tributaries (Meade (1996); Meade and Moody (2010)).

The scenario that removes the main stem Missouri reservoirs includes the removal of Lewis and Clarke Lake and the Gavins Point Dam. Lewis and Clarke Lake has a reservoir capacity of approximately 0.67 km^3 (Lehner et al., 2011) accounting for only 0.8% of the total reservoirs capacity removed in the Missouri scenario. In the first run, Lewis and Clarke Lake was not removed which resulted in an average annual sediment transport at Tarbert Landing of only 50.5 MT/y. The removal of Lewis and Clarke Lake therefore generates a difference of 15.1 MT/y at Tarbert Landing. Meade and Moody (2010) state that directly after construction of the Gavins Point dam the suspended sediment load downstream of the dam declined from 160 MT/y to 50 MT/y. The conclusion can therefore be drawn that although the reservoir capacity is fairly small Lewis and Clarke Lake is a major sediment sink.

6.5 Recommendations

1. Find a method to include sediment production by bank erosion of the river channels and evaluate how this contributes to the total sediment transport in the Mississippi.
2. Evaluate sediment production in more detail and produce a map that includes local differences.
3. The dams that are incorporated in the model were derived from the GRanD database. Although this is the most comprehensive database there are still dams missing. A clear example that could influence the outcome of this research is the Fort Randall Dam, which is located in the Missouri river. According to the research of Meade and Moody (2010), the closure of this dam in 1953 resulted in a decline in sediment load from 160 MT/y in 1952 to 50 MT/y 1953. The absence of this dam and other dams in the database and in the model can therefore influence the outcome of the simulation results. Finding the missing dams and including them into the model could therefore lead to better results.

Chapter 7

Conclusions

In the last decades, several types of river engineering structures and measures were implemented and constructed in the Mississippi River. As a result of the construction of these human modifications, the suspended sediment load has declined significantly from an annual average of approximately 400 MT/yr to an average of 110 MT/yr in the period 1987-2006 (Meade & Moody, 2010). Many articles state that the primary source of this reduction in suspended sediment transport is the construction of reservoirs and dams (Keown et al. (1986); Kesel and Yodis (1992); Meade and Moody (2010); Horowitz (2010)). This reduction in sediment transport has resulted in the degradation of wetlands and coastal zones, extensive land loss and increased flood risks in the delta, which will only become more severe in the future as a result of climate change, subsidence and sea-level rise. In this research, a quantitative model of the suspended sediment flux in the Mississippi River was developed using the PCR-GLOBWB model with the aim to identify the basin-wide effect of reservoir construction on sediment transport. To model the suspended sediment flux in the Mississippi, the mechanisms behind sediment trapping in reservoirs were identified and developed into equations that could be included in PCR-GLOBWB. To calculate the sedimentation in the reservoirs, the equation developed by Camp (1945) was used, which assumes quiescent flow with steady state discharge, complete mixing and no resuspension in an ideal rectangular flow basin or settling tank. With this equation, the trapping efficiency of a reservoir can be quantified based on the actual settling velocity and the critical settling velocity, which can be derived from the incoming discharge and reservoir surface area.

The relative error between the literature and the PCR-GLOBWB model was on average 2.5 at Tarbert Landing and Herman for the scenario with reservoirs. At Clinton the relative error was relatively high with a value of 6.7, while at Olmsted it was relatively low with an average of 2. The high error found at Clinton can be caused by a large underestimation of the sediment production in the Upper-Mississippi catchment or by an inaccuracy in the source data. The relative error of the model is primarily caused by the assumption that the sediment production of an entire subcatchment was constant in space and time. Furthermore, the model does not make a distinction between different types of erosion and therefore neglects the effect of local differences and extreme conditions. The current model can be improved by incorporating the process of bank erosion in more detail, local differences in sediment production and a variable sediment production over time.

The year-to-year variability significantly declines if the reservoirs are introduced at Clinton, Hermann and Tarbert Landing. This decline in year-to-year variability is likely caused by the regulating effect of the reservoirs, which results in a more constant discharge throughout the year by decreasing the peak discharge and increasing the minimum discharge. The Ohio River is an exception, as the year-to-year variability at Olmsted is relatively constant over time for the scenario with and without reservoirs. This can be caused by a less regulating effect of the reservoirs

the more constant discharge trend of the Ohio River (which shows less extremes than the other tributaries). The seasonal variability in the discharge and sediment transport at Tarbert Landing and Hermann declines significantly if the reservoirs are introduced for normal and extreme years. The lower seasonal variability is caused by the storage capacity of the reservoirs, which lowers and delays the maximum discharge and increases the minimum discharge. The sediment transport shows a significant decline if the reservoirs are introduced, as the storage capacity of the reservoirs does not only alter the seasonal variability but also the magnitude due to trapping.

The sediment transport along the entire Mississippi River and its tributaries declined significantly when the reservoirs were introduced. The greatest decline could be observed in the main channel of the Missouri and the Lower-Mississippi. The decline in the tributaries was relatively small in comparison to the rivers and main channels, this is probably caused by the smaller trapping efficiency of the reservoirs located in the tributaries. The importance of the tributaries was emphasized by comparing the difference between the actual and potential sediment transport between the upstream and downstream part of the Missouri and Ohio River. The introduction of the reservoirs has resulted in a decline of the actual sediment transport along the river system, as less of the available sediment is routed downstream. The introduction of the reservoirs does not effect the contribution of the Great Plains to the MRB, as for both scenarios (with and without reservoirs) most of the available sediment is routed downstream.

The model was run for 5 different scenarios which included: the removal of all reservoirs (1), no reservoirs (2), the main stem Missouri reservoirs (3), the reservoirs with a surface area larger than 100 km^2 (4) and the main stem Ohio River reservoirs (5). The average annual sediment transport at Tarbert Landing declined with 62% if the reservoirs were included. The scenario that includes the removal of the 8 main stem Missouri reservoirs, resulted in the smallest relative decline in comparison to the scenario without reservoirs, resulting in a relative decline of only 24.2% at Hermann and 40.3% at Tarbert Landing, while the scenario that included the removal of 34 large reservoirs resulted in a relative decline of 50.8% at Hermann and 49.3% at Tarbert Landing. Thus, although the exclusion of the large reservoirs removes more than twice as much reservoir capacity as the scenario that excludes the main stem Missouri reservoirs, the effects on the sediment transport at Tarbert Landing are minor. One of the biggest sediment sinks in the Missouri River is Lewis and Clarke Lake and the Gavins Point Dam, which generate a difference of 15.1 MT/yr at Tarbert Landing although it has a reservoir capacity of only 0.67 km^3 which account for only 0.8% of the total reservoir capacity that is removed in the Missouri scenario. The model can be improved by verifying if there are dams and reservoirs missing from the model. The current reservoirs and dams were derived from the GRanD database and although this is one of the most comprehensive databases for reservoir attributes, there are still dams missing.

References

Alexander, J. S., Wilson, R. C. & Green, W. R. (2012). *A brief history and summary of the effects of river engineering and dams on the mississippi river system and delta.* US Department of the Interior, US Geological Survey. 4, 8, 9, 10, 12

Berelson, W. L., Caffrey, P. A. & Hamerlinck, J. D. (2004). Mapping hydrologic units for the national watershed boundary dataset. *JAWRA Journal of the American Water Resources Association*, *40*(5), 1231–1246. 31

Blum, M. D. & Roberts, H. H. (2009). Drowning of the mississippi delta due to insufficient sediment supply and global sea-level rise. *Nature Geoscience*, *2*(7), 488. 1, 13, 14

Borland, W. M. (1971). Reservoir sedimentation. *River Mechanics*, *2*, 29–1. 21

Brown, C. B. (1944). *The control of reservoir silting* (No. 521). US Govt. print. off. 17

Brune, G. M. (1953). Trap efficiency of reservoirs. *Eos, Transactions American Geophysical Union*, *34*(3), 407–418. 17, 18, 19, 20, 23

Camp, T. R. (1945). Sedimentation and the design of settling tanks. In *Proceeding of ASCE* (Vol. 71). 22, 30, 59

Chen, C.-N. (1975). Design of sediment retention basins. In *Proceedings of the national symposium on urban hydrology and sediment control, july 28-31, 1975.* 22, 23

Chow, V., Maidment, D. & Mays, L. (1988). Applied hydrology, 572 pp. *Editions McGraw-Hill, New York*. 26

Churchill, M. (1948). Discussion of "analysis and use of reservoir sedimentation data". *Proceedings of the Federal Interagency Sedimentation Conference. Bureau of Reclamation, US Department of the Interior, Washington, DC (pp. 139-140)*. 20, 21, 23

Court, A. (1974). The climate of the conterminous united states. *Climates of North America. World Survey of Climatology. Vol. 11*, 193–343. 5

CPRA. (2012). Restoration authority of louisiana (2012) louisiana's comprehensive master plan for a sustainable coast. *Coastal Protection and Restoration Authority of Louisiana. Baton Rouge, LA*. 14

CPRA. (2017). Restoration authority of louisiana (2017) louisiana's comprehensive master plan for a sustainable coast. *Coastal Protection and Restoration Authority of Louisiana. Baton Rouge, LA*. 1, 14, 15, 65

Galat, D. L. & Lipkin, R. (2000). Restoring ecological integrity of great rivers: historical hydrographs aid in defining reference conditions for the missouri river. *Hydrobiologia*, *422*, 29–48. 13

Gill, M. A. (1979). Sedimentation and useful life of reservoirs. *Journal of Hydrology*, *44*(1-2), 89–95. 19

Haan, C. T., Barfield, B. J. & Hayes, J. C. (1994). *Design hydrology and sedimentology for small catchments.* Elsevier. 21, 22

Hargrove, W. L., Johnson, D., Snethen, D. & Middendorf, J. (2010). From dust bowl to mud bowl: Sedimentation, conservation measures, and the future of reservoirs. *Journal of soil and water conservation*, *65*(1), 14A–17A. 17

Heinemann, H. G. (1981). A new sediment trap efficiency curve for small reservoirs. *Journal of the American Water Resources Association*, *17*(5), 825–830. 17, 19, 20

Heinemann, H. G., Sprague, L. A. & Blevins, D. W. (2011). *Trends in suspended-sediment loads and concentrations in the mississippi river basin, 1950–2009* (Tech. Rep.). US Geological Survey. 37, 38, 39, 51, 55, 56, 57

Horowitz, A. J. (2010). A quarter century of declining suspended sediment fluxes in the mississippi river and the effect of the 1993 flood. *Hydrological Processes*, *24*(1), 13–34. 1, 11, 31, 37, 38, 39, 40, 55, 56, 59

Jacobson, R. B., Blevins, D. W. & Bitner, C. J. (2009). Sediment regime constraints on river restoration—an example from the lower missouri river. *Geological Society of America Special Papers*, *451*, 1–22. 12, 13

Keown, M. P., Dardeau, E. A. & Causey, E. M. (1986). Historic trends in the sediment flow regime of the mississippi river. *Water Resources Research*, *22*(11), 1555–1564. 1, 7, 10, 11, 12, 27, 37, 38, 51, 59

Kesel, R. H. (2003). Human modifications to the sediment regime of the lower mississippi river flood plain. *Geomorphology*, *56*(3), 325–334. 1, 7, 12, 13, 55, 57

Kesel, R. H. & Yodis, E. G. (1992). Some effects of human modifications on sand-bed channels in southwestern mississippi, usa. *Environmental Geology*, *20*(2), 93–104. 1, 11, 59

Kim, W., Mohrig, D., Twilley, R., Paola, C. & Parker, G. (2009). Is it feasible to build new land in the mississippi river delta? *EOS, Transactions American Geophysical Union*, *90*(42), 373–374. 15

Knox, J. C. (2007). The mississippi river system. *Large rivers: geomorphology and management*, 145–182. 3, 4, 5, 6

Kummu, M., Lu, X., Wang, J. & Varis, O. (2010). Basin-wide sediment trapping efficiency of emerging reservoirs along the mekong. *Geomorphology*, *119*(3-4), 181–197. 20

Lehner, B., Liermann, C. R., Revenga, C., Vörösmarty, C., Fekete, B., Crouzet, P., ... others (2011). High-resolution mapping of the world's reservoirs and dams for sustainable river-flow management. *Frontiers in Ecology and the Environment*, *9*(9), 494–502. 8, 9, 30, 58, 67

Lehner, B., Verdin, K. & Jarvis, A. (2008). New global hydrography derived from spaceborne elevation data. *Eos, Transactions American Geophysical Union*, *89*(10), 93–94. 30

Leopold, L. B. & Maddock, T. (1953). *The hydraulic geometry of stream channels and some physiographic implications* (Vol. 252). US Government Printing Office. 29

Loos, S., Middelkoop, H., van der Perk, M. & van Beek, R. (n.d.). Estimating large scale seasonal sediment yields with a process based approach an global datasets. 55

Meade, R. H. (1996). Setting: Geology, hydrology, sediments, and engineering of the mississippi river. *US Geological Survey (USGS)*, 13–30. 3, 10, 58

Meade, R. H. & Moody, J. A. (2010). Causes for the decline of suspended-sediment discharge in the mississippi river system, 1940–2007. *Hydrological Processes*, *24*(1), 35–49. 1, 2, 5, 11, 12, 31, 37, 38, 56, 57, 58, 59

Morton, R. A. (2008). Historical changes in the mississippi-alabama barrier-island chain and the roles of extreme storms, sea level, and human activities. *Journal of Coastal Research*, 1587–1600. 14

Mossa, J. (1996). Sediment dynamics in the lowermost mississippi river. *Engineering Geology*, *45*(1-4), 457–479. 1, 57

Paola, C., Twilley, R. R., Edmonds, D. A., Kim, W., Mohrig, D., Parker, G., ... Voller, V. R. (2011). Natural processes in delta restoration: Application to the mississippi delta. *Annual Review of Marine Science*, *3*, 67–91. 13

Parker, R. (1988). Uncertainties in defining the suspended sediment budget for large drainage basins. *IN: Sediment Budgets. IAHS Publication*(174). 11

Thonon, I., Roberti, J. R., Middelkoop, H., Van der Perk, M. & Burrough, P. A. (2005). In situ measurements of sediment settling characteristics in floodplains using a lisst-st. *Earth Surface Processes and Landforms*, *30*(10), 1327–1343. 30

USAEWES. (1930). Sediment investigations on the mississippi river and its tributaries prior to 1930. *Pap. H, Vicksburg*. 7

USDA. (1954). Inventory of published and unpublished sediment-load data in the united states. *Sediment. Bull. I, Soil. Conserv. Service, Washington D.C.*. 7

Van Beek, L. & Bierkens, M. F. (2009). The global hydrological model pcr-globwb: conceptualization, parameterization and verification. *Utrecht University, Utrecht, The Netherlands*. 1, 25, 26, 27

Verstraeten, G. & Poesen, J. (2000). Estimating trap efficiency of small reservoirs and ponds: methods and implications for the assessment of sediment yield. *Progress in Physical Geography*, *24*(2), 219–251. 17, 18, 20, 21, 23

Vörösmarty, C. J., Meybeck, M., Fekete, B., Sharma, K., Green, P. & Syvitski, J. P. (2003). Anthropogenic sediment retention: major global impact from registered river impoundments. *Global and planetary change*, *39*(1-2), 169–190. 20

Ward, P. R. (1980). Sediment transport and a reservoir siltation formula for zimbabwe-rhodesia. *Civil Engineer in South Africa*, *22*(1), 9–15. 20

Wisser, D., Frolking, S., Hagen, S. & Bierkens, M. F. (2013). Beyond peak reservoir storage? a global estimate of declining water storage capacity in large reservoirs. *Water Resources Research*, *49*(9), 5732–5739. 17, 20

Appendix A

Environmental drivers

Table A.1: Environmental drivers for different CPRA scenarios (CPRA, 2017).

Scenario	Precipitation	Evapotranspiration	Sea-level rise	Subsidence rate	Storm frequency	Average storm intensity
Low	-5% decline in 50-year cumulative precipitation compared to historical data	-30% of 50-yr cumulative Penman-Monteith evapotranspiration	0.14 m over 50 years	0 to 19 [mm/yr]	-28% change of current frequency	+10% of current central pressure deficit
Medium	Historical monthly average	Historic Penman-Monteith monthly mean evapotranspiration record	0.49 m over 50 years	0 to 19 [mm/yr]	-14% change of current frequency	+12,5% of current central pressure deficit
High	14% increase in 50-year cumulative precipitation compared to historical data	Historic Penman-Monteith monthly mean evapotranspiration record	0.83 m over 50 years	0 to 25 [mm/yr]	0% change	+15% of current central pressure deficit

Appendix B

Overview of removed dams and reservoirs for each of the developed scenarios

Table B.1: Overview of removed dams and reservoirs for each of the scenarios described in Section 4.4 derived from the GRanD database (Lehner et al., 2011).

Main Missouri reservoirs removed		Large reservoirs removed		Main Ohio reservoirs removed	
Grand ID	Dam name	Grand ID	Dam name	Grand ID	Dam name
307	Fort Peck Dam	307	Fort Peck Dam	1665	Willow Island Lock and Dam
328	Holter Dam	753	Garrison Dam	1747	Smithland Lock and Dam
332	Hauser Dam	758	Winnibigoshish Dam	1753	Kentucky Dam
753	Garrison Dam	767	Leech Lake Dam	1797	Watts Bar
870	Oahe Dam	870	Oahe Dam	1822	Chickamauga
884	Big Bend Dam	884	Big Bend Dam	1824	Pickwick Landing
895	Gavins Point Dam	913	Kingsley	1829	Nickajack
966	Marshall Creek Dam	989	Harry S. Truman Dam	1835	Wheeler
11402	Lewis and Clarke Lake	993	Bagnell Dam	1847	Gunterville
		1026	Table Rock Dam		
		1029	Pensacola		
		1032	Oologah Lake		
		1036	Bull Shoals		
		1067	Greers Ferry		
		1075	Robert S. Kerr Lock and Dam		
		1077	Eufaula Lake		
		1112	Blakely Mountain Dam		
		1135	Denison Dam		
		1181	Iron Bridge Dam		
		1230	Joe B. Hogsett Dam		
		1238	Richland Creek Dam		
		1269	Toledo Bend		
		1275	Sam Rayburn Dan		
		1287	Livingstone Dam		
		1752	Barkley Dam		
		1753	Kentucky		
		1756	Wolf Creek		
		1797	Watts Bar		
		1822	Chickamauga		
		1824	Pickwick Landing		
		1835	Wheeler		
		1847	Guntersville		
		1848	Sardis Dam		
		1869	Grenada Dam		